Control of Time-Delay Interconnected Nonlinear Systems under Input Saturations: A Broad Learning System-Based Approach

Moshu Qian[a], Chenglin Sun[a], Cunsong Wang[a], Xinggang Yan[b] and, Cuimei Bo[a]

[a] College of Electrical Engineering and Control Science, Nanjing Tech University, Nanjing, 211816, China; [b] Instrumentation and Control Research Group, University of Kent, Canterbury, Kent CT2 7NT, UK

ARTICLE HISTORY
Compiled December 12, 2023

ABSTRACT
In this paper, the adaptive control problem is investigated for a class of interconnected nonlinear systems (INS) with unknown interconnection delays and input saturations. For state unmeasurable problem, a full dimension state observer (SO) is designed to estimate the inaccessible state variables. Broad learning system (BLS), a novel nonlinear approximation technique, is introduced in this study to identify the unknown dynamics and could achieve better approximation performance. An adaptive distributed control (DC) scheme is proposed for the uncertain time-delay INS without input saturation, which guarantees that the stability of the closed loop INS. On this basis, the input saturation problem is further considered, an online approximation smooth function is added into the distributed adaptive tracking controller, such that the closed-loop INS have the anti-input saturation capability. In terms of Lyapunov theory, all the signals in the closed-loop uncertain time-delay INS with input saturation are proved to be uniformly ultimately bounded (UUB) and the tracking errors could converge to a small neighbourhood of zero. Finally, one simulation example performed on two parallel inverted pendulum cars demonstrates the superiority of the developed distributed control scheme.

KEYWORDS
Interconnected nonlinear systems (INS), distributed control (DC), input saturation, time-delay interconnection.

1. Introduction

In recent years, the INS are becoming more and more important in the fields of modern control theory and application, which could be used to describe the modern complex cyber-physical systems, such as chemical reaction systems, power networks systems, collaborative robotic arms and so on. Due to huge application potential of INS, the control synthesis and stability analyzes problem of INS has been attracted the great attention from many scholars (Mu, 2018; Salari, 2019; Yu, 2019; Zhang & Xiang, 2022), meanwhile it also brings the great challenge (Li & Yang, 2018; Zhao, 2020). Because the adaptive control has been extensively studied, it is considered for INS firstly. (Sui, 2021) investigates adaptive neural network (NN)-based controller design for stochastic nonlinear systems with unmodeled dynamics in finite-time prescribed performance. An

CONTACT Moshu Qian. Email: moshu_qian@126.com.

adaptive tracking control approach for a class of nonlinear state-constrained and time-varying delay systems is proposed using Nussbaum gain technique in (Li, 2018). The observer-based adaptive fuzzy controller is discussed for nonlinear systems with input constraints and unknown disturbance in (Zhang, 2020). However, the above results are not suitable to the INS composed of multiple subsystems but a single nonlinear system.

Recently, some important results for the INS have been reported. In (Wang & Yang, 2019), the decentralized control strategy is studied for interconnected systems with input quantization by using a static event triggered mechanism. In (Ma & Ma, 2020), the decentralized fault tolerant controller is designed for a switched large scale systems. In (Zhang, 2020), the fault detection and control issue is discussed for the INS by designing the decentralized controller. A decentralized tracking proportional-integral (PI) controller is investigated in (Sun & Zong, 2020) for INS with input quantization. By introducing a reinforcement learning algorithm, (Liu, 2019) studies the optimal decentralized control issue for the interconnected systems. In the above discussion, all the control schemes are decentralized, which cannot achieve the cooperative control of INS utilizing the neighbor's information.

To date, the distributed control (DC) technique has a large number of applications in the field of multi-agent systems (MASs), such as in (Li & Zheng, 2023) an adaptive fuzzy prescribed-time distributed control problem is presented for non-strict feedback nonlinear MASs. Further, in (Li & Li, 2023) the event triggered mechanism is added for the distributed finite time formation controller to reduce the communication cost. The results of MASs only makes use of the exchanged information, however, the results of the interconnected systems depend on both the exchanged information and transmission substance between the subsystems. Thus they are different. Recently, a DC scheme is developed for linear interconnected systems by using linear matrix inequalities (LMIs) in (Zhang, 2019), and a separation principle is employed for a class of distributed interconnected systems in (Yang, 2019), but both of them are designed for only linear interconnected systems.

The time-delay interconnected functions may occur because INS always consist of many interacted subsystems and complex coupling relationships. For example, the time-delays are generated from the transmission of reaction materials, electrical energy, force and torque in chemical reaction systems, power networks systems, collaborative robotic arms, respectively. There are some research results, (Yoo, 2016) investigates the time-delay interconnected functions for INS. (Sun & Hou, 2020) proposes a tracking control strategy for the time delay INS. Besides, the inputs of the above systems are material flow, power and motor speed, they are constrained within a certain range due to the physical or energy limitations of actuators, which leads to the input saturations. There also exist some results, (Zhan & Sui, 2021) designs a fuzzy decentralised controller for the fractional-order INS with input saturation. (Chen, 2020) studies the finite time controller for linear interconnected systems with input saturation. The input saturation and interconnection delays have not been studied simultaneously in above interconnected systems, especially when the states are unknown, it will be more difficult. Therefore, how to simultaneously compensate the delayed interconnections, input saturations when the states are unknown and further achieve the robust performance of the INS is still a challenge.

Motivated by the above problems, this paper is concerned with the distributed tracking control problem for a class of time-delay INS with input saturations. To solve these problems, the broad learning system, a smooth variant Sigmoid function and Lyapunov-Krasovskii theory are introduced into the controller design procedure. Si-

multaneously, a state observer is designed for each subsystem to estimated partial inaccessible state variables. The main contributions of this study are concluded as follows.
(i) Compared with the decentralized tracking control scheme, in which the interconnected information is not adapted for the controller design, a novel DC approach is proposed in this study for a class of time-delay INS by introducing the interconnected information into the controller of each subsystem, and it can achieve the cooperative control of INS.
(ii) Compared with the other intelligent methods, such as convolutional neural network (CNNs), fuzzy logic system (FLS), RBFNNs and the single layer feedforward neural networks, broad learning system (BLS) is employed as another approximator to identify the unknown dynamics in this study, and it could improve the approximation accuracy and learning time by the structure of the random vector functional link neural network and adding the enhancement nodes into the output layer.
(iii) Simultaneously, the unknown time delay interconnection and input saturations problem of INS is solved in this study, which greatly extends the existing practical engineering applications. The difficulty caused by unknown time delay interconnection with unknown upper bounds is solved by designing the novel Lyapunov- Krasovskii functions. The difficulty caused by the input saturation constraints is overcome by introducing a smooth variant Sigmoid function.

The remainder of this paper is organized as follows. In section 2, the preliminaries and problem formulation are given. In section 3, the adaptive distributed fault tolerant tracking control scheme is proposed, and then the stability of closed loop systems is analyzed. The simulation results are given in section 4 to verify the effectiveness of the proposed control approach. Finally, some conclusions are given in section 5.

2. Preliminaries and problem formulation

2.1. Preliminaries

The broad learning system (BLS) is the novel neural network structure with approximation capabilities. The simplified broad learning systems are displayed as Figure 1, where only b enhancement neurons are used in the framework. Assume that there are K_i feature neurons in the i_{th} feature subset, the m feature mappings are adopted to collect the feature of n inputs, the mapped feature node Z_i is denoted as (Chu, 2020)

$$Z_i = \zeta_1(XW_{ei} + B_{ei}),\ i = 1, ..., m \tag{1}$$

where $X \in R^{1\times n}$ denotes the input vector, Z^i is represented as $Z^m = [Z_1, \ldots, Z_m]$, $B_{ei} \in R^{1\times K_i}$ and $W_{ei} \in R^{n\times K_i}$ are the width and randomly weight at the initiation of neural network. ζ_1 is a preset activation function.

The j_{th} enhancement node is yielded

$$H_j = \zeta_2(Z^m W_{bj} + B_{bj}),\ j = 1, ..., b \tag{2}$$

where $B_{bj} \in R$ and $W_{bj} \in R^{K_1+...+K_m}$ are the width and randomly weight, respectively. ζ_2 is a preset activation function.

Besides, the value of i and j is decided by the complexity of the neural network systems, here the enhanced neuron vector is set as $H = [H_1, \ldots, H_b]$. The output of

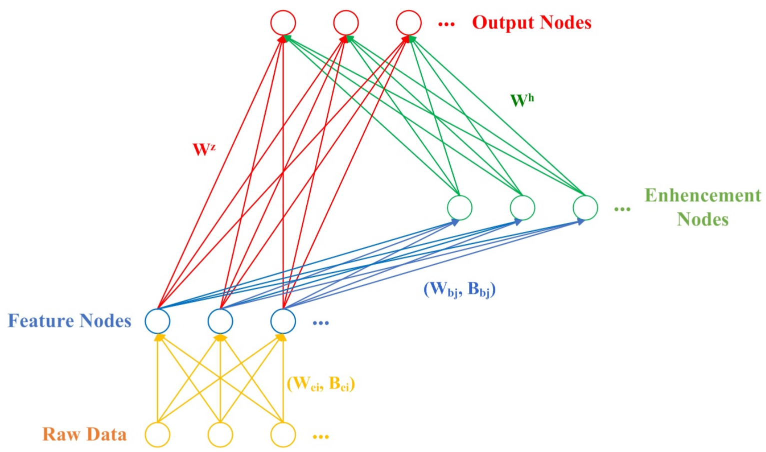

Figure 1. The structure of BLS.

BLS neural network is denoted as

$$Y(X|W) = (Z^m W^z + HW^h)^T = W^T \varphi = \varphi^T W \tag{3}$$

where $Y \in R$ denotes the output of BLS neural network. $W^z \in R^{K_1+K_2+\ldots+K_m}$ and $W^h \in R^b$ are the width and randomly weight, respectively. $W = [W^z;\ W^h]$ denotes the approximated weight column vector. $\varphi = [Z^m; H]$, $\varphi \in R^{K_1+K_2\ldots+K_m+b}$ is a function of X. Since φ is determined by the input X, BLS with weight W and variable X can estimate any continuous vector function uniformly (Chu, 2020; Sui, 2020).

The optimal weight vector is chosen as

$$W^* = \text{arg}\mathbf{min}_{W\in\Omega}[\sup_{X\in U} \|Y(X|W) - F\|] \tag{4}$$

where Y is employed to estimate the unknown dynamics F.

The estimation error can be denoted as

$$\epsilon = F - Y(X|W^*) \tag{5}$$

where F is the approximated vector, $|\epsilon_j| \leq \bar{\epsilon}$ and $\bar{\epsilon}$ is an unknown positive constant.

From (3)-(5), it is concluded that

$$F = W^{*T}\varphi + \epsilon \tag{6}$$

Then the approximated error of F is

$$F - Y(X|\hat{W}) = \tilde{W}^T \varphi + \epsilon \tag{7}$$

where $\tilde{W} = W^* - \hat{W}$, and $\hat{W}$ is the estimated value of W^*.

Definition 1 (Zhan & Sui, 2021): The variant Sigmoid function $\mathcal{S}(x)$ could be described as

$$\mathcal{S}(x) = \frac{c_1}{e^{-c_2 x} + 1} - c_3 \tag{8}$$

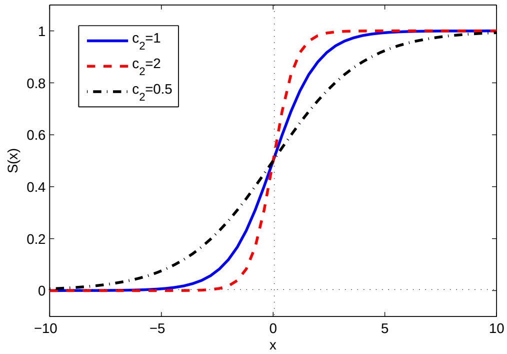

Figure 2. Variant sigmoid function with $c_1 = 1, c_3 = 0$.

where c_1, c_2, and c_3 are positive constants to be designed.

Remark 1: In Definition 1, $\mathcal{S}(x)$ is a differentiable real function and has no singularity. Meanwhile, Taylor expansion of $\mathcal{S}(x)$ is always convergent (Yan, 2021). For example, $\mathcal{S}(.)$ with $c_1 = 1, c_3 = 0$ is illustrated as Figure 2.

Lemma 1 (Sun & Hou, 2020): If a set $\Gamma := \{Z||Z| < 0.8814\varsigma\}$, then any Z does not belong to Γ such that the following inequality holds.

$$1 - 2\tanh^2(Z/\varsigma) \leq 0,\ \varsigma > 0.$$

Lemma 2 (Sun & Hou, 2020): There exists a constant $\nu > 0$ such that $\lim_{s\to 0}\tanh^2(s/\nu)/s = 0$ holds where $s \in R$ is a variable.

2.2. *Problem formulation*

Consider the general nonlinear time-delay interconnected nonlinear systems, consisting of N interconnection subsystems with unknown nonlinearities (Baigzadehnoe, 2020; Sun & Hou, 2020)

$$\begin{cases} \dot{x}_{i,m} = x_{i,m+1} + f_{i,m}(x_i) + g_{i,m}(y) + h_{i,m}(y_{\tau_{i,m}}), \\ \qquad m = 1, 2, \cdots, n_i - 1 \\ \dot{x}_{i,n_i} = u_i + f_{i,n_i}(x_i) + g_{i,n_i}(y) + h_{i,n_i}(y_{\tau_{i,n_i}}) \\ \qquad y_i = x_{i,1} \\ \qquad x_i(t) = \psi_i(t), \quad -\bar{d}_i \leq t \leq 0 \end{cases} \tag{9}$$

where $x_i = [x_{i,1}, x_{i,2}, \ldots, x_{i,n_i}]^T$, $x_i \in R^{n_i}$ is the state vector of the ith subsystem, $y_i \in R$ is the output signal of the ith subsystem, $u_i \in R$ is the control input of the ith subsystem. $f_{i,j}(\cdot)$ $(i = 1, \cdots, N; j = 1, \cdots, n_i)$ is the ith subsystem unknown nonlinear term. $g_{i,j}(y)$ with $y = [y_1, \ldots, y_N]^T$ is the unknown nonlinear interconnection terms connecting the i_{th} subsystem with the other subsystems while $h_{i,j}(y_{\tau_{i,j}})$ with $y_{\tau_{i,j}} = [y_1(t - \tau_{i,j,1}(t)), \ldots, y_N(t - \tau_{i,j,N}(t))]^T$ indicates the unknown time delay nonlinear interconnection effects among subsystems. $\tau_{i,j,k}$ $(k = 1, \ldots, N)$ is the unknown time varying delay in $h_{i,j}(\cdot)$ and $y_k(t - \tau_{i,j,k}(t))$ is the delayed output signal of the k_{th} subsystem received by the ith subsystem. $\psi_i(t)$ indicates the initial state vector function of the i_{th} subsystem. It is considered that $d_{i,j}(t) = \max_{1\leq j\leq n_i, 1\leq k\leq N}\{\tau_{i,j,k}(t)\}$,

$|d_{i,j}(t)| \le \bar{d}_i$ and $\bar{d}_i$ is a positive constant (Baigzadehnoe, 2020).

Assumption 1 (Baigzadehnoe, 2020; Sun & Hou, 2020): The derivative of $d_{i,j}(t)$ is bounded with a known positive constant d_i^*, and $\dot{d}_{i,j} \le d_i^* \le 1$.

Assumption 2 (Zhang, 2020): The unknown nonlinear interconnection function $g_{i,j}(y)$ satisfies

$$\|g_{i,j}(y)\| \le \sum_{k=1}^{N} \phi_{i,j,k}(y_k)$$

where $\phi_{i,j,k}(\cdot)$ $(j = 1, \cdots, n_i)$ is partially known class-$\mathcal{K}$ function and satisfies

$$|\phi_{i,j,k}(\xi) - \check{\phi}_{i,j,k}(\xi)| \le \bar{\phi}_{i,j,k}(\xi), \ \forall \xi \in \mathbb{R}$$

$\check{\phi}_{i,j,k}(\xi)$ is the nominal function of $\phi_{i,j,k}(\xi)$, and the unknown function $\bar{\phi}_{i,j,k}(\xi)$ denotes the bound on uncertainty for $\phi_{i,j,k}(\xi)$.

Assumption 3 (Yoo, 2016): It is assumed that the delayed interconnection function $h_{i,j}(y_{\tau_{i,j}})$ satisfies

$$\|h_{i,j}(y_{\tau_{i,j}})\| \le \sum_{k=1}^{N} \omega_{i,j,k}(y_k(t - d_{i,j}))$$

where $\omega_{i,j,k}(\cdot)$ is partially known class-$\mathcal{K}$ function and satisfies

$$|\omega_{i,j,k}(\xi) - \check{\omega}_{i,j,k}(\xi)| \le \bar{\omega}_{i,j,k}(\xi), \ \forall \xi \in \mathbb{R}$$

the nominal function of $\omega_{i,j,k}(\xi)$ is indicated as $\check{\omega}_{i,j,k}(\xi)$ and the unknown function $\bar{\omega}_{i,j,k}(\xi)$ denotes the bound on uncertainty for $\omega_{i,j,k}(\xi)$.

The control objective of this study is to design a broad learning system (BLS) approximator based adaptive distributed tracking control scheme, such that the output $y_i(t)$ of the nonstrict-feedback interconnected nonlinear time-delay systems (9) follows the command signal $y_{i,r}(t)$ and all the signals in the closed-loop interconnected systems are uniformly ultimately bounded (UUB).

Remark 2: For practical systems, the interconnection delay is time-varying and bounded in most cases. In many practical applications, the derivative of interconnection delay is also bounded, namely the change of interconnection delay is slow. Thus, d_i^* is accordingly assumed to be known and bounded in Assumption 1. Besides, three nonlinear functions are considered to make the proposed distributed approach more applicable and general in this study. The first unknown nonlinearity $f_{i,j}(.) \in R$ is the function of the state x_i and could be approximated by adopting the well-known universal approximator. To deal with the second nonlinear interconnection function $g_{i,j}(.)$ without losing generality, Assumption 2 is accordingly employed. Besides, the function boundary represented by Assumption 3 is utilized to compensate the third nonlinear delayed interconnection function $h_{i,j}(.)$ in this paper. It is worth noting that Assumptions 1-3 are common in the field of interconnected systems (Ghosh, 2009; Sun & Hou, 2020; Tong, 2011; Yoo, 2016).

3. Distributed tracking controller design

3.1. Distributed controller design without input saturations

To deal with inaccessible state variables, a state observer could be designed for interconnected systems (9) as follows

$$\dot{\hat{x}}_{i,m} = \hat{x}_{i,m+1} - l_{i,m}(\hat{x}_{i,1} - y_i), m = 1, ..., n_i - 1 \quad (10)$$
$$\dot{\hat{x}}_{i,n_i} = u_i - l_{i,n_i}(\hat{x}_{i,1} - y_i) \quad (11)$$

where the estimation of x_i is indicated as $\hat{x}_i = [\hat{x}_{i,1}, \hat{x}_{i,2}, \ldots, \hat{x}_{i,n_i}]^T$. $l_{i,j}(j = 1 \ldots, n_i)$ is the observer gain parameter, which should be selected to make the following matrix

$$A_{i,c} = \begin{bmatrix} -l_{i,1} & & & \\ \vdots & & I_{i,n_i-1} & \\ -l_{i,n_i} & 0 & \ldots & 0 \end{bmatrix} \quad (12)$$

is a strict Hurwitz matrix, I_{i,n_i-1} is the $n_i - 1$ dimension unit matrix. That is, there exist two positive definite matrices P_i, Q_i, such that

$$P_i A_{i,c} + A_{i,c}^T P_i = -Q_i \quad (13)$$

Defining the observer errors as $e_{i,j} = x_{i,j} - \hat{x}_{i,j}$, one has

$$\dot{e}_{i,m} = -l_{i,m}e_{i,1} + e_{i,m+1} + f_{i,m}(x_i) + g_{i,m}(y) + h_{i,m}(y_{\tau_{i,m}}) \quad (14)$$
$$\dot{e}_{i,n_i} = -l_{i,n_i}e_{i,1} + f_{i,n_i}(x_i) + g_{i,n_i}(y) + h_{i,n_i}(y_{\tau_{i,n_i}}) \quad (15)$$

which can be expressed as the following form

$$\dot{e}_i = A_{i,c}e_i + F_i(x_i) + G_i(y) + H_i(y_{\tau_i}) \quad (16)$$

where $e_i = [e_{i,1}, \ldots, e_{i,n_i}]^T$, $G_i(y) = [g_{i,1}(y), \ldots, g_{i,n_i}(y)]^T$, $F_i(x_i) = [f_{i,1}(x_i), \ldots, f_{i,n}(x_i)]^T$, $H_i(y_{\tau_i}) = [h_{i,1}(y_{\tau_{i,1}}), \ldots, h_{i,n_i}(y_{\tau_{i,n_i}})]^T$.

Remark 3: In the interconnected nonlinear systems (INS), some state variables could not be inaccessible owing to the constraints of cost, space and other conditions. However, in the most existing research results, all state variables of INS are required to be known, such as (Chu, 2020; Liu, 2019; Yang, 2019). Compared with these results, in which all state variables of the considered interconnected systems are measurable and could be used to feedback control design, the partial state variables of the considered interconnected systems are allowed to be unmeasured in this paper, which could be identified by designing the state observer. Thus, the problem discussed in our study is more complicated and tough to solve in term of the existing results.

Choose the Lyapunov-Krasovskii functional $V_i = V_i^1 + V_i^2$ to analyse the stability of the ith closed loop subsystem, V_i^1 includes the observer errors and time delay interconnected term effects, V_i^2 is defined later.

$$V_i^1 = \frac{1}{2}e_i^T P_i e_i + V_{h_i} \quad (17)$$

with

$$V_{h_i} = \frac{N\beta}{1-d_i^*}\sum_{j=1}^{n_i} e^{\chi_i \bar{d}_i}\int_{t-d_{i,j}}^{t} e^{-\chi_i(t-\vartheta)}\left(\sum_{k=1}^{N}\omega_{i,j,k}^2(y_k(\vartheta))\right)\mathrm{d}\vartheta$$

where the parameters $\beta > 0,\ \chi_i > 0$ will be determined later.

Differentiating V_i^1 in (17) along the trajectory of (16) yields

$$\dot{V}_i^1 = -\frac{1}{2}e_i^T Q_i e_i + e_i^T P_i F(x_i) + e_i^T P_i G_i(y) + e_i^T P_i H_i(y_{\tau_i}) + \dot{V}_{h_i} \tag{18}$$

Taking the time derivative of V_{h_i} yields

$$\begin{aligned}\dot{V}_{h_i} &= -\chi_i V_{h_i} + \frac{N\beta}{1-d_i^*}\sum_{j=1}^{n_i} e^{\chi_i \bar{d}_i}\left(\sum_{k=1}^{N}\omega_{i,j,k}^2(y_k)\right) - \frac{N\beta}{1-d_i^*}\sum_{j=1}^{n_i} e^{\chi_i \bar{d}_i} \\ &\quad \left((1-\dot{d}_{i,j})e^{-\chi_i d_{i,j}}\sum_{k=1}^{N}\omega_{i,j,k}^2(y_k(t-d_{i,j}))\right) \\ &\le -\chi_i V_{h_i} + \frac{N\beta}{1-d_i^*}\sum_{j=1}^{n_i} e^{\chi_i \bar{d}_i}\left(\sum_{k=1}^{N}\omega_{i,j,k}^2(y_k)\right) - N\beta\sum_{j=1}^{n_i}\sum_{k=1}^{N}\omega_{i,j,k}^2(y_k(t-d_{i,j}))\end{aligned} \tag{19}$$

According to Assumption 3, it could be seen that

$$\begin{aligned}e_i^T P_i H_i(y_{\tau_i}) + \dot{V}_{h_i} &\le \delta\|P_i\|^2 e_i^2 + \beta\|H_i(y_{\tau_i})\|^2 + \dot{V}_{h_i} \\ &\le \delta\|P_i\|^2 e_i^2 + N\beta\sum_{j=1}^{n_i}\sum_{k=1}^{N}\omega_{i,j,k}^2(y_k(t-d_{i,j})) + \dot{V}_{h_i} \\ &\le \delta\|P_i\|^2 e_i^2 - \chi_i V_{h_i} + \frac{N\beta}{1-d_i^*}\sum_{j=1}^{n_i} e^{\chi_i \bar{d}_i}\left(\sum_{k=1}^{N}\omega_{i,j,k}^2(y_k)\right) \\ &\le \delta\|P_i\|^2 e_i^2 - \chi_i V_{h_i} + \frac{N\beta}{1-d_i^*}\sum_{j=1}^{n_i} e^{\chi_i \bar{d}_i}\left(\sum_{k=1}^{N}(\breve{\omega}_{i,j,k}(y_k)+\bar{\omega}_{i,j,k}(y_k))^2\right) \\ &\le \delta\|P_i\|^2 e_i^2 - \chi_i V_{h_i} + \frac{N\beta}{1-d_i^*}\sum_{j=1}^{n_i} e^{\chi_i \bar{d}_i}\left(\sum_{k=1}^{N}2\breve{\omega}_{i,j,k}^2(y_k)\right) \\ &\quad + \frac{N\beta}{1-d_i^*}\sum_{j=1}^{n_i} e^{\chi_i \bar{d}_i}\left(\sum_{k=1}^{N}2\bar{\omega}_{i,j,k}^2(y_k)\right)\end{aligned} \tag{20}$$

where $\delta > 0$ is a small positive scalar and $\beta = \frac{1}{4\delta}$.

Substituting (20) into (18) yield

$$
\begin{aligned}
\dot{V}_i^1 \leq & -\frac{1}{2}e_i^T Q_i e_i + e_i^T P_i F(x_i) + e_i^T P_i G_i(y) + \delta\|P_i\|^2 e_i^2 - \chi_i V_{h_i} \\
& + \frac{N\beta}{1-d_i^*}\sum_{j=1}^{n_i} e^{\chi_i \bar{d}_i}\left(\sum_{k=1}^{N} 2\breve{\omega}_{i,j,k}^2(y_k)\right) + \frac{N\beta}{1-d_i^*}\sum_{j=1}^{n_i} e^{\chi_i \bar{d}_i}\left(\sum_{k=1}^{N} 2\bar{\omega}_{i,j,k}^2(y_k)\right) \\
\leq & -\frac{1}{2}e_i^T Q_i e_i + e_i^T P_i F(x_i) - \chi_i V_{h_i} + 2\delta\|P_i\|^2 e_i^2 + \beta G_i^2(y) \\
& + \frac{N\beta}{1-d_i^*}\sum_{j=1}^{n_i} e^{\chi_i \bar{d}_i}\left(\sum_{k=1}^{N} 2\breve{\omega}_{i,j,k}^2(y_k)\right) + \frac{N\beta}{1-d_i^*}\sum_{j=1}^{n_i} e^{\chi_i \bar{d}_i}\left(\sum_{k=1}^{N} 2\bar{\omega}_{i,j,k}^2(y_k)\right) \\
\leq & -\frac{1}{2}e_i^T Q_i e_i + 2\delta\|P_i\|^2 e_i^2 + e_i^T P_i F(x_i) + N\beta\sum_{j=1}^{n_i}\sum_{k=1}^{N}\phi_{i,j,k}^2(y_k) - \chi_i V_{h_i} \\
& + \frac{N\beta}{1-d_i^*}\sum_{j=1}^{n_i} e^{\chi_i \bar{d}_i}\left(\sum_{k=1}^{N} 2\breve{\omega}_{i,j,k}^2(y_k)\right) + \frac{N\beta}{1-d_i^*}\sum_{j=1}^{n_i} e^{\chi_i \bar{d}_i}\left(\sum_{k=1}^{N} 2\bar{\omega}_{i,j,k}^2(y_k)\right) \\
\leq & -\frac{1}{2}e_i^T Q_i e_i + 2\delta\|P_i\|^2 e_i^2 + e_i^T P_i F(x_i) + N\beta\sum_{j=1}^{n_i}\sum_{k=1}^{N} 2\breve{\phi}_{i,j,k}^2(y_k) \\
& + N\beta\sum_{j=1}^{n_i}\sum_{k=1}^{N} 2\bar{\phi}_{i,j,k}^2(y_k) - \chi_i V_{h_i} + \frac{N\beta}{1-d_i^*}\sum_{j=1}^{n_i} e^{\chi_i \bar{d}_i}\left(\sum_{k=1}^{N} 2\breve{\omega}_{i,j,k}^2(y_k)\right) \\
& + \frac{N\beta}{1-d_i^*}\sum_{j=1}^{n_i} e^{\chi_i \bar{d}_i}\left(\sum_{k=1}^{N} 2\bar{\omega}_{i,j,k}^2(y_k)\right) \\
\leq & -\frac{1}{2}e_i^T Q_i e_i + 3\delta\|P_i\|^2 e_i^2 + \beta\sum_{j=1}^{n_i} f_{i,j}^T(x_i) f_{i,j}(x_i) + N\beta\sum_{j=1}^{n_i}\sum_{k=1}^{N} 2\breve{\phi}_{i,j,k}^2(y_k) \\
& + N\beta\sum_{j=1}^{n_i}\sum_{k=1}^{N} 2\bar{\phi}_{i,j,k}^2(y_k) - \chi_i V_{h_i} + \frac{N\beta}{1-d_i^*}\sum_{j=1}^{n_i} e^{\chi_i \bar{d}_i}\left(\sum_{k=1}^{N} 2\breve{\omega}_{i,j,k}^2(y_k)\right) \\
& + \frac{N\beta}{1-d_i^*}\sum_{j=1}^{n_i} e^{\chi_i \bar{d}_i}\left(\sum_{k=1}^{N} 2\bar{\omega}_{i,j,k}^2(y_k)\right) \qquad (21)
\end{aligned}
$$

Choosing a positive definite matrix Λ_i such that $Q_i = 6\delta\|P_i\|^2 I_{n_i} + 2\Lambda_i$, then

$$\begin{aligned}\dot{V}_i^1 \le -\chi_i e_i^2 - \chi_i V_{h_i} + \beta \sum_{j=1}^{n_i} f_{i,j}^T(x_i) f_{i,j}(x_i) + N\beta \sum_{j=1}^{n_i}\sum_{k=1}^{N} 2\check{\phi}_{i,j,k}^2(y_k) \\ +N\beta \sum_{j=1}^{n_i}\sum_{k=1}^{N} 2\bar{\phi}_{i,j,k}^2(y_k) + \frac{N\beta}{1-d_i^*}\sum_{j=1}^{n_i} e^{\chi_i \bar{d}_i}\left(\sum_{k=1}^{N} 2\check{\omega}_{i,j,k}^2(y_k)\right) \\ +\frac{N\beta}{1-d_i^*}\sum_{j=1}^{n_i} e^{\chi_i \bar{d}_i}\left(\sum_{k=1}^{N} 2\bar{\omega}_{i,j,k}^2(y_k)\right)\end{aligned} \tag{22}$$

where χ_i is the minimum eigenvalue of Λ_i.

In this position, a distributed tracking controller will be designed for the considered nonlinear system (9).

Step 1: Consider the first equation

$$\dot{y}_i = \hat{x}_{i,2} + e_{i,2} + f_{i,1}(x_i) + g_{i,1}(y) + h_{i,1}(y_{\tau_{i,1}}) \tag{23}$$

The tracking error is defined as $z_{i,1} = y_i - y_{i,r}$, the derivative of $z_{i,1}$ is obtained as

$$\begin{aligned}\dot{z}_{i,1} &= \hat{x}_{i,2} + e_{i,2} + f_{i,1}(x_i) + g_{i,1}(y) + h_{i,1}(y_{\tau_{i,1}}) - \dot{y}_{i,r} \\ &= z_{i,2} + \alpha_{i,1} + e_{i,2} + f_{i,1}(x_i) + g_{i,1}(y) + h_{i,1}(y_{\tau_{i,1}}) - \dot{y}_{i,r}\end{aligned} \tag{24}$$

where $z_{i,2} = \hat{x}_{i,2} - \alpha_{i,1}$, $\alpha_{i,1}$ is the first virtual control input of the ith subsystem to be determined later.

The quadratic Lyapunov function is selected as

$$V_{i,1}^2 = \frac{1}{2} z_{i,1}^2 + V_{h_{i,1}} \tag{25}$$

where $V_{h_{i,1}} = \frac{N}{1-d_i^*} e^{\chi_i \bar{d}_i} \int_{t-d_{i,1}}^{t} e^{-\chi_i(t-\vartheta)} \left(\sum_{k=1}^{N} \omega_{i,1,k}^2(y_k(\vartheta))\right) \mathrm{d}\vartheta$.
Differentiating $V_{i,1}^2$ in (25) along the trajectory of (24) yields

$$\begin{aligned}\dot{V}_{i,1}^2 = z_{i,1}^T \dot{z}_{i,1} + \dot{V}_{h_{i,1}} = z_{i,1}(z_{i,2} + \alpha_{i,1} \\ +e_{i,2} + f_{i,1}(x_i) + g_{i,1}(y) + h_{i,1}(y_{\tau_{i,1}}) - \dot{y}_{i,r}) + \dot{V}_{h_{i,1}}\end{aligned} \tag{26}$$

According to Assumption 2, one yields

$$\begin{aligned} z_{i,1} g_{i,1}(y) \le |z_{i,1}||g_{i,1}(y)| \le |z_{i,1}| \sum_{k=1}^{N} \phi_{i,1,k}(y_k) \\ \le \frac{1}{4} z_{i,1}^2 + (\sum_{k=1}^{N} \phi_{i,1,k}(y_k))^2 \le \frac{1}{4} z_{i,1}^2 + N \sum_{k=1}^{N} (\phi_{i,1,k}(y_k))^2 \\ \le \frac{1}{4} z_{i,1}^2 + N \sum_{k=1}^{N} |\phi_{i,1,k}(y_k) - \check{\phi}_{i,1,k}(y_k) + \check{\phi}_{i,1,k}(y_k)|^2 \end{aligned}$$

$$\leq \frac{1}{4}z_{i,1}^2 + N\sum_{k=1}^{N} 2|\phi_{i,1,k}(y_k) - \check{\phi}_{i,1,k}(y_k)|^2 + N\sum_{k=1}^{N} 2|\check{\phi}_{i,1,k}(y_k)|^2$$

$$\leq \frac{1}{4}z_{i,1}^2 + N\sum_{k=1}^{N} 2\check{\phi}_{i,1,k}^2(y_k) + N\sum_{k=1}^{N} 2\bar{\phi}_{i,1,k}^2(y_k)$$

According to Assumption 3, one yields

$$z_{i,1}h_{i,1}(y_{\tau_{i,1}}) \leq |z_{i,1}||h_{i,1}(y_{\tau_{i,1}})| \leq |z_{i,1}|\sum_{k=1}^{N}\omega_{i,1,k}(y_k(t-d_{i,1}))$$

$$\leq \frac{1}{4}z_{i,1}^2 + (\sum_{k=1}^{N}\omega_{i,1,k}(y_k(t-d_{i,1})))^2 \leq \frac{1}{4}z_{i,1}^2 + N\sum_{k=1}^{N}\omega_{i,1,k}^2(y_k(t-d_{i,1}))$$

According to Young's inequality, the inequality could be derived as

$$z_{i,1}e_{i,2} \leq \frac{1}{2}z_{i,1}^2 + \frac{1}{2}\|e_{i,2}\|^2. \tag{27}$$

Taking the time derivative of $V_{h_{i,1}}$ yields

$$\begin{aligned}\dot{V}_{h_{i,1}} &= -\chi_i V_{h_{i,1}} + \frac{N}{1-d_i^*}e^{\chi_i\bar{d}_i}\left(\sum_{k=1}^{N}\omega_{i,1,k}^2(y_k) - (1-\dot{d}_{i,1})e^{-\chi_i d_{i,1}}\sum_{k=1}^{N}\omega_{i,j,k}^2(y_k(t-d_{i,1}))\right)\\
&\leq -\chi_i V_{h_{i,1}} + \frac{N}{1-d_i^*}e^{\chi_i\bar{d}_i}\left(\sum_{k=1}^{N}2\check{\omega}_{i,1,k}^2(y_k)\right) - N\sum_{k=1}^{N}\omega_{i,1,k}^2(y_k(t-d_{i,1}))\\
&\quad + \frac{N}{1-d_i^*}e^{\chi_i\bar{d}_i}\left(\sum_{k=1}^{N}2\bar{\omega}_{i,1,k}^2(y_k)\right)\end{aligned} \tag{28}$$

Substituting (27)-(28) into (26) yields

$$\begin{aligned}\dot{V}_{i,1}^2 &\leq z_{i,1}(z_{i,2} + \alpha_{i,1} + f_{i,1}(x_i) - \dot{y}_{i,r}) + \frac{1}{2}e_{i,2}^2 + N\sum_{k=1}^{N}2\check{\phi}_{i,1,k}^2(y_k) + N\sum_{k=1}^{N}2\bar{\phi}_{i,1,k}^2(y_k)\\
&+ z_{i,1}^2 - \chi_i V_{h_{i,1}} + \frac{N}{1-d_i^*}e^{\chi_i\bar{d}_i}\left(\sum_{k=1}^{N}2\check{\omega}_{i,1,k}^2(y_k)\right) + \frac{N}{1-d_i^*}e^{\chi_i\bar{d}_i}\left(\sum_{k=1}^{N}2\bar{\omega}_{i,1,k}^2(y_k)\right)\end{aligned} \tag{29}$$

From the above inequality, the virtual control input could be designed as

$$\alpha_{i,1} = -b_{i,1}z_{i,1} + \dot{y}_{i,r} \tag{30}$$

where $b_{i,1} > 0$ is a constant.

Substituting (30) into (29) yields

$$\dot{V}_{i,1}^2 \leq -(b_{i,1} - \frac{3}{2})z_{i,1}^2 + z_{i,1}^T z_{i,2} + \frac{1}{2}f_{i,1}^2(x_i) + N\sum_{k=1}^{N}2\check{\phi}_{i,1,k}^2(y_k) + N\sum_{k=1}^{N}2\bar{\phi}_{i,1,k}^2(y_k)$$

$$-\chi_i V_{h_{i,1}} + \frac{1}{2}e_{i,2}^2 + \frac{N}{1-d_i^*}e^{\chi_i \bar{d}_i}\left(\sum_{k=1}^{N} 2\breve{\omega}_{i,1,k}^2(y_k)\right) + \frac{N}{1-d_i^*}e^{\chi_i \bar{d}_i}\left(\sum_{k=1}^{N} 2\bar{\omega}_{i,1,k}^2(y_k)\right)$$

Step 2: Define the error as $z_{i,2} = \hat{x}_{i,2} - \alpha_{i,1}$, the derivative of $z_{i,2}$ is obtained as

$$\dot{z}_{i,2} = z_{i,3} + \alpha_{i,2} - l_{i,2}(\hat{x}_{i,1} - y_i) - \dot{\alpha}_{i,1}$$

where $z_{i,3} = \hat{x}_{i,3} - \alpha_{i,2}$, $\alpha_{i,2}$ is the second virtual control input of the ith subsystem to be determined later.

The quadratic Lyapunov function is selected as

$$V_{i,2}^2 = V_{i,1}^2 + \frac{1}{2}z_{i,2}^2 \tag{31}$$

Taking the derivative of (31) yields

$$\dot{V}_{i,2}^2 = \dot{V}_{i1}^2 + z_{i,2}^T(z_{i,3} + \alpha_{i,2} - l_{i,2}(\hat{x}_{i,1} - y_i) - \dot{\alpha}_{i,1}) \tag{32}$$

The virtual control input could be designed as

$$\alpha_{i,2} = -z_{i,1} - b_{i,2}z_{i,2} + \dot{\alpha}_{i,1} - l_{i,2}e_{i,1} \tag{33}$$

where $b_{i,2} > 0$ is a constant.

Substituting (33) into (32) yields

$$\begin{aligned}\dot{V}_{i,2}^2 \leq& -(b_{i,1} - \frac{3}{2})z_{i,1}^2 - b_{i,2}z_{i,2}^2 + z_{i,2}^T z_{i,3} + \frac{1}{2}f_{i,1}^2(x_i) - \chi_i V_{h_{i,1}} + \frac{1}{2}e_{i,2}^2 \\ &+N\sum_{k=1}^{N} 2\breve{\phi}_{i,1,k}^2(y_k) + N\sum_{k=1}^{N} 2\bar{\phi}_{i,1,k}^2(y_k) + \frac{N}{1-d_i^*}e^{\chi_i \bar{d}_i}\left(\sum_{k=1}^{N} 2\breve{\omega}_{i,1,k}^2(y_k)\right) \\ &+\frac{N}{1-d_i^*}e^{\chi_i \bar{d}_i}\left(\sum_{k=1}^{N} 2\bar{\omega}_{i,1,k}^2(y_k)\right)\end{aligned} \tag{34}$$

Step m: Define the error as $z_{i,m} = \hat{x}_{i,m} - \alpha_{i,m-1}$, the derivative of $z_{i,m}$ is obtained as

$$\dot{z}_{i,m} = -\dot{\alpha}_{i,m-1} + l_{i,m}e_{i,1} + \alpha_{i,m} + z_{i,m+1} \tag{35}$$

where $z_{i,m+1} = \hat{x}_{i,m+1} - \alpha_{i,m}$ $(m = 3, \ldots, n_i - 1)$, $\alpha_{i,m}$ is the mth virtual control input of the ith subsystem to be determined later.

The quadratic Lyapunov function is selected as

$$V_{i,m}^2 = V_{i,m-1}^2 + \frac{1}{2}z_{i,m}^2 \tag{36}$$

Calculating the derivative of $V_{i,m}^2$ yields

$$\dot{V}_{i,m}^2 = \dot{V}_{i,m-1}^2 + z_{i,m}(z_{i,m+1} + \alpha_{i,m} + l_{i,m}e_{i,1} - \dot{\alpha}_{i,m-1}) \tag{37}$$

The virtual input could be designed as

$$\alpha_{i,m} = -z_{i,m-1} - b_{i,m} z_{i,m} + \dot{\alpha}_{i,m-1} - l_{i,m} e_{i,1} \tag{38}$$

where $b_{i,m} > 0$ is a constant.

Substituting (38) into (37) yields

$$\begin{gathered}
\dot{V}_{i,m}^2 \leq -(b_{i,1} - \frac{3}{2}) z_{i,1}^2 - \sum_{c=2}^{m} b_{i,c} z_{i,c}^2 + z_{i,m}^T z_{i,m+1} \\
+\frac{1}{2} e_{i,2}^2 + \frac{1}{2} f_{i,1}^2(x_i) - \chi_i V_{h_{i,1}} + N \sum_{k=1}^{N} 2\check{\phi}_{i,1,k}^2(y_k) + N \sum_{k=1}^{N} 2\bar{\phi}_{i,1,k}^2(y_k) \\
+\frac{N}{1-d_i^*} e^{\chi_i \bar{d}_i} \left(\sum_{k=1}^{N} 2\check{\omega}_{i,1,k}^2(y_k) \right) + \frac{N}{1-d_i^*} e^{\chi_i \bar{d}_i} \left(\sum_{k=1}^{N} 2\bar{\omega}_{i,1,k}^2(y_k) \right)
\end{gathered}$$

Step n_i: Define the error as $z_{i,n_i} = \hat{x}_{i,n_i} - \alpha_{i,n_i-1}$, the derivative of z_{i,n_i} is obtained as

$$\dot{z}_{i,n_i} = u_i - l_{i,n_i}(\hat{x}_{i,1} - y_i) - \dot{\alpha}_{i,n_i-1} \tag{39}$$

The quadratic Lyapunov function is selected as

$$V_i^2 = V_{i,n_i-1}^2 + \frac{1}{2} z_{i,n_i}^2 \tag{40}$$

Taking the time derivative of V_i^2 yields

$$\begin{gathered}
\dot{V}_i^2 = \dot{V}_{i,n_i-1}^2 + z_{i,n_i}(u_i + l_{i,n_i} e_{i,1} - \dot{\alpha}_{i,n_i-1}) \\
= -(b_{i,1} - \frac{3}{2}) z_{i,1}^2 - \sum_{c=2}^{n_i-1} b_{i,c} z_{i,c}^2 + z_{i,n_i-1}^T z_{i,n_i} + \frac{1}{2} e_{i,2}^2 + \frac{1}{2} f_{i,1}^2(x_i) - \chi_i V_{h_{i,1}} \\
+N \sum_{k=1}^{N} 2\check{\phi}_{i,1,k}^2(y_k) + N \sum_{k=1}^{N} 2\bar{\phi}_{i,1,k}^2(y_k) + \frac{N}{1-d_i^*} e^{\chi_i \bar{d}_i} \left(\sum_{k=1}^{N} 2\check{\omega}_{i,1,k}^2(y_k) \right) \\
+\frac{N}{1-d_i^*} e^{\chi_i \bar{d}_i} \left(\sum_{k=1}^{N} 2\bar{\omega}_{i,1,k}^2(y_k) \right) + z_{i,n_i}(u_i + l_{i,n_i} e_{i,1} - \dot{\alpha}_{i,n_i-1})
\end{gathered} \tag{41}$$

For the ith subsystem of (9), the following Lyapunov function is defined as

$$V_i = V_i^1 + V_i^2 \tag{42}$$

Taking the derivative of V_i yields

$$\begin{gathered}
\dot{V}_i \leq -(\chi_i - \frac{1}{2}) e_i^2 + \gamma_i - 2\chi_i V_{h_i} - (b_{i,1} - \frac{3}{2}) z_{i,1}^2 - \sum_{c=2}^{n_i-1} b_{i,c} z_{i,c}^2 + z_{i,n_i-1}^T z_{i,n_i} \\
+\eta_i + z_{i,n_i}(u_i + l_{i,n_i} e_{i,1} - \dot{\alpha}_{i,n_i-1})
\end{gathered}$$

$$\leq -(\chi_i - \frac{1}{2})e_i^2 + 2\tanh^2(z_{i,n_i}/\varsigma)(\gamma_i + \eta_i) - 2\chi_i V_{h_i} - (b_{i,1} - \frac{3}{2})z_{i,1}^2 - \sum_{c=2}^{n_i-1} b_{i,c} z_{i,c}^2$$
$$+z_{i,n_i-1}^T z_{i,n_i} + z_{i,n_i}(u_i + l_{i,n_i} e_{i,1} - \dot{\alpha}_{i,n_i-1}) + (1 - 2\tanh^2(z_{i,n_i}/\varsigma))(\gamma_i + \eta_i) \quad (43)$$

where the unknown dynamics are $\eta_i(x_i) = \beta \sum_{j=1}^{n_i} f_{i,j}^T(x_i) f_{i,j}(x_i) + N\beta \sum_{j=1}^{n_i} \sum_{k=1}^{N} 2\bar{\phi}_{i,j,k}^2(y_k) + N \sum_{k=1}^{N} 2\bar{\phi}_{i,1,k}^2(y_k) + \frac{N\beta}{1-d_i^*} \sum_{j=1}^{n_i} e^{\chi_i \bar{d}_i}(\sum_{k=1}^{N} 2\bar{\omega}_{i,j,k}^2(y_k)) + \frac{N}{1-d_i^*} e^{\chi_i \bar{d}_i}(\sum_{k=1}^{N} 2\bar{\omega}_{i,1,k}^2(y_k)) + \frac{1}{2} f_{i,1}^2(x_i)$. And the lumped nominal functions are $\gamma_i = N\beta \sum_{j=1}^{n_i} \sum_{k=1}^{N} 2\check{\phi}_{i,j,k}^2(y_k) + \frac{N\beta}{1-d_i^*} \sum_{j=1}^{n_i} e^{\chi_i \bar{d}_i} \left(\sum_{k=1}^{N} 2\check{\omega}_{i,j,k}^2(y_k)\right) + N \sum_{k=1}^{N} 2\check{\phi}_{i,1,k}^2(y_k) + \frac{N}{1-d_i^*} e^{\chi_i \bar{d}_i}(\sum_{k=1}^{N} 2\check{\omega}_{i,1,k}^2(y_k))$. It is easily concluded that $\eta_i + \gamma_i > 0$. $\varsigma > 0$ is a constant.

To eliminate the adverse effect of the unknown dynamics, the broad learning system (3) is employed and $\eta_i(x_i) = W_i^{*T} \varphi_i$ where W_i^* is the optimal weight and φ_i is the basis function. Accordingly it can be seen that $\hat{\eta}_i(\hat{x}_i) = \hat{W}_i^T \varphi_i$ and $\tilde{\eta}_i = \tilde{W}_i^T \varphi_i$, where $\hat{\eta}_i$ and $\hat{W}_i$ are the estimated values of η_i and W_i^*, their estimation errors are $\tilde{\eta}_i = \eta_i - \hat{\eta}_i$ and $\tilde{W}_i = W_i^* - \hat{W}_i$.

From Lemma 2, the adaptive distributed tracking controller is designed as

$$u_i = -z_{i,n_i-1} - b_{i,n_i} z_{i,n_i} + \dot{\alpha}_{i,n_i-1} - l_{i,n_i} e_{i,1} - \frac{2}{z_{i,n_i}}(\tanh^2(z_{i,n_i}/\varsigma)(\gamma_i + \hat{\eta}_i)) \quad (44)$$

where $b_{i,n} > 0$ is a constant.

The adaptive parameter update law is

$$\dot{\hat{W}}_i = \frac{1}{\varrho_i}(2\tanh^2(z_{i,n_i}/\varsigma)\varphi_i - \lambda_i \hat{W}_i), \ i = 1, 2, ..., N \quad (45)$$

where λ_i is a positive constant.

The calculation steps of broad learning system (BLS) neural networks for the above approximated parameter $\hat{\eta}$ are listed in Tables 1-2, where $X = [\hat{x}^T]$, $\hat{\eta}(0)$ and $\hat{W}(0)$ are the initial values of $\hat{\eta}$ and $\hat{W}$, respectively.

For the ith closed loop subsystem, the following Lyapunov function is chosen as

$$\bar{V}_i = V_i + \frac{1}{2}\varrho_i \tilde{W}_i^T \tilde{W}_i \quad (46)$$

where ϱ_i is a positive constant.

Substituting (43)-(44) into $\dot{\bar{V}}_i$, when $t \to \infty$, the following inequality holds

$$\dot{\bar{V}}_i \leq -(\chi_i - \frac{1}{2})e_i^2 - 2\chi_i V_{h_i} - (b_{i,1} - \frac{3}{2})z_{i,1}^2 - \sum_{c=2}^{n_i} b_{i,c} z_{i,c}^2 + 2\tanh^2(z_{i,n_i}/\varsigma)\tilde{W}_i^T \varphi_i$$
$$+(1 - 2\tanh^2(z_{i,n_i}/\varsigma))(\gamma_i + \eta_i) + 2\tanh^2(z_{i,n_i}/\varsigma)\bar{\epsilon} - \varrho_i \tilde{W}_i^T \dot{\hat{W}}_i \quad (47)$$

Remark 4: In this study, BLS is employed as a novel approximator to identify the effect of the unknown dynamics. Compared with the convolutional networks approximation technique, which suffers from the time consuming training process because of a great number of hyperparameters and complicated structures, BLS effectively eliminates the drawback of the long training process (Chen, 2019). Further, the mathematical proof of the universal approximation property of BLS has also been provided

Table 1. The initial algorithm of broad learning systems

The initial algorithm
Input: X;
Output: $\hat{\eta}(0)$;
for i=1, i$\leq$ m;
$\vert$Random W_{ei}, B_{ei};
$\vert$Calculate $Z_i = \zeta_1(XW_{ei} + B_{ei})$;
end;
Set $Z^m = [Z_1, ..., Z_m]$;
for j=1, $j \leq b$;
$\vert$Random W_{bj}, B_{bj};
$\vert$Calculate $H_j = \zeta_2(Z^m W_{bj} + B_{bj})$;
end;
Set $H = [H_1, ..., H_b]$;
Random W^z, W^h;
Set $\hat{W}(0) = [W^z; W^h]$, $\varphi^T = [Z^m, H]$;
Set $\hat{\eta}(0) = \hat{W}^T(0)\varphi$;

Table 2. The process algorithm of broad learning systems

The process algorithm
Input: $X, \hat{W}$;
Output: $\hat{\eta}$;
for i=1, i$\leq$ m;
$\vert$Calculate $Z_i = \zeta_1(XW_{ei} + B_{ei})$;
end;
Set $Z^m = [Z_1, ..., Z_m]$;
for j=1, $j \leq b$;
$\vert$Calculate $H_j = \zeta_2(Z^m W_{bj} + B_{bj})$;
end
Set $H = [H_1, ..., H_b]$;
Set $\varphi^T = [Z^m, H]$;
Set $\hat{\eta} = \hat{W}^T\varphi$;

in (Chen, 2019). Moreover, different from fuzzy logic system (FLS), RBFNNs and the single layer feedforward neural networks approximation techniques, which usually are more sensitive to the parameter settings and suffer from slow convergence (Chen & Liu, 2018; Cui, 2019; Niu, 2021; Sui, 2020) , BLS has achieved breakthrough successes in identifying the uncertain nonlinear systems based on the structure of the random vector functional link neural network and adding extra enhancing nodes (Sui, 2020).

Based on the above descriptions, the following result is now ready to be presented.

Theorem 1. Under Assumptions 1-3, consider the interconnected systems (9) with interconnection delays, a distributed tracking controller (44) and the adaptive parameter update algorithm (45) guarantees that the nonlinear time-delay interconnected systems (9) are uniformly ultimate bounded stable, meanwhile, all tracking errors of (9) are also uniformly ultimately bounded (UUB).

Proof. For the whole closed-loop interconnected systems, the following Lyapunov candidate function are chosen as

$$V = \sum_{i=1}^{N} \bar{V}_i \tag{48}$$

From Lemma 1 and (43), $(1 - 2\tanh^2(z_{i,n_i}/\varsigma))(\gamma_i + \eta_i) \leq 0$ is obtained and then

$$\begin{aligned}\dot{V} \leq \sum_{i=1}^{N}(-(\chi_i - \frac{1}{2})e_i^2 - 2\chi_i V_{h_i} - (b_{i,1} - \frac{3}{2})z_{i,1}^2 - \sum_{c=2}^{n_i} b_{i,c} z_{i,c}^2 - \frac{\lambda_i}{2}\tilde{W}_i^2 \\ + \frac{\lambda_i}{2}W_i^2 + 2\tanh^2(z_{i,n_i}/\varsigma)\bar{\epsilon}) \leq -\mu V + M\end{aligned} \tag{49}$$

where $\mu = \min_{i=1,\ldots,N}\{(2\chi_i - 1), 2\chi_i, 2b_{i,1} - 3, 2b_{i,c}, \frac{\lambda_i}{\varrho_i}\}$, $\chi_i > 1/2$, $b_{i,1} > \frac{3}{2}$, $b_{i,c} > 0$, $(c = 2, \ldots, n_i)$, $M \geq \|M_0\|$ is a upper bound constant of the time varying function M_0 with

$$M_0 = \sum_{i=1}^{N}(\frac{\lambda_i}{2}W_i^T W_i + 2\tanh^2(z_{i,n_i}/\varsigma)\bar{\epsilon})$$

From (49), one yields

$$V \leq V(0)e^{-\mu t} + \frac{M}{\mu}(1 - e^{-\mu t}) \tag{50}$$

That is

$$V \leq V(0)e^{-\mu t} + \frac{M}{\mu} \tag{51}$$

Select the appropriate parameters to make $\mu > 0$ and $M > 0$, then on the basis of (51), it is clear that $e_{i,j}$, $z_{i,j}$, $\tilde{W}_i$ $(i = 1, ..., N;\ j = 1, \ldots, n_i)$ of systems (9) are uniformly ultimately bounded (UUB). Simultaneously, the whole closed-loop INS are UUB stable. From (49), $b_{i,j} > 0$, $\lambda_i > 0$, $\varsigma > 0$, and $\varrho_i > 0$ are properly chosen to make $z_{i,1}$ converge to a small region near origin. Namely, the larger μ and smaller M, the better control performance of (9). Moreover, the output tracking error of i_{th} subsystem $z_{i,1} = y_i - y_{ir}$ satisfies

$$\sum_{i=1}^{N}\frac{z_{i,1}^2}{2} \leq V(0)e^{-\mu t} + \frac{M}{\mu} \tag{52}$$

According to the above inequality, it is easy to obtain $|z_{i,1}| \leq \sqrt{2V(0)e^{-\mu t}} + \sqrt{\frac{2M}{\mu}}$. Therefore, $z_{i,1}$ can be adjusted into a small neighborhood of the origin through properly choosing the parameters $b_{i,j}$, χ_i, λ_i and ϱ_i. This completes the proof.

Remark 5: Different from the general nonlinear or switched systems (Liu, 2020; Wang, 2020, 2021; Zhan & Sui, 2021), which could only describe one plant, the considered nonlinear interconnected systems (9) could describe N different plants, which

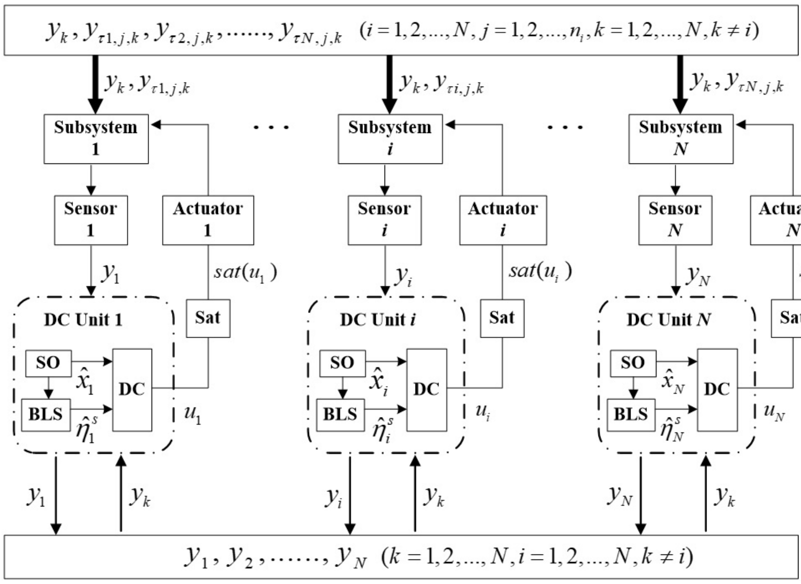

Figure 3. Block diagram of the distributed control systems

will cooperative control to complete a large and complex task. Compared with the existing research results of interconnected systems (Liu, 2019; Sun & Zong, 2020; Zhang & Xiang, 2022), which did not consider the time-delay interconnection, the nonlinear time-delay problem is investigated in this study. By using the upper bound information of time-delay functions $\frac{N\beta}{1-d_i^*}\sum_{j=1}^{n_i} e^{\chi_i \bar{d}_i}\left(\sum_{k=1}^{N} 2\breve{\omega}_{i,j,k}^2(y_k)\right)$ in the controller (44), a distributed tracking control scheme is developed to eliminate the adverse effect of interconnection delay and further guarantee the stability of the whole interconnected systems.

3.2. Distributed controller design with input saturations

Actually, the input saturation is a class of the most critical constraints and always occurs in the actual physical systems. There are two main motivations to research the input saturation constraint. One is that input saturation is a potential factor degrades the control system performance, which often leads to undesirable inaccuracy, or even causes system unstable. Another is that the energy or magnitude is always limited in practice, so the saturation constraint of the control input is necessary.

$$\begin{cases} \dot{x}_{i,m} = x_{i,m+1} + f_{i,m}(x_i) + g_{i,m}(y) + h_{i,m}(y_{\tau_{i,m}}), \\ \qquad m = 1, 2, \cdots, n_i - 1 \\ \dot{x}_{i,n_i} = \mathrm{sat}(u_i) + f_{i,n_i}(x_i) + g_{i,n_i}(y) + h_{i,n_i}(y_{\tau_{i,n_i}}) \\ \qquad y_i = x_{i,1} \\ x_i(t) = \psi_i(t), -\bar{d}_i \le t \le 0 \end{cases} \tag{53}$$

Then under the input saturation constraint, the control variable u_i of the interconnected systems (9) is transformed into

$$\mathrm{sat}(u_i) = \begin{cases} \mathrm{sign}(u_i)u_{iM}, & |u_i(t)| \geq u_{iM} \\ u_i, & |u_i(t)| < u_{iM} \end{cases} \tag{54}$$

where $u_{iM} > 0$ is the bound of u_i. Clearly, there is a sharp corner between the ideal input command u_i and the actual input $\mathrm{sat}(u_i)$ when $|u_i| \geq u_{iM}$. Thus the above backstepping control approach cannot be directly applied. From Definition 1, a smooth function could be adopted to approximate the input saturation

$$A_i(u_i) = u_{iM} \times (2\mathcal{S}(\frac{a_0 u_i}{u_{iM}}) - 1) \tag{55}$$

where $\mathcal{S}(.)$ is a variant sigmoid function with $c_1 = 1, c_2 = 1, c_3 = 0$, and a_0 is a positive designed constant. For example, the curve of the input saturation approximation under $u(t) = sin(t), a_0 = 3, u_M = 0.6$ is shown in Figure 5.

Then the approximated error could be

$$\Delta_i(u_i) = \mathrm{sat}(u_i) - A_i(u_i) = u_{iM} + \mathrm{sat}(u_i) - (u_{iM} \times 2\mathcal{S}(\frac{a_0 u_i}{u_{iM}})) \tag{56}$$

It is noted that $\Delta_i(u_i)$ is bounded with

$$\Delta_i(u_i) = |\mathrm{sat}(u_i) - A_i(u_i)| \leq |u_{iM} + \mathrm{sat}(u_i)| + |u_{iM} \times 2\mathcal{S}(\frac{a_0 u_i}{u_{iM}})| \leq 4u_{iM} \tag{57}$$

Consider the mean-value theorem (Apostol, 1958), and there exists a positive constant $0 < \vartheta_i < 1$ such that

$$A_i(u_i) = A_i(u_{i0}) + A_{i,u_{i\vartheta}}(u_i - u_{i0}) \tag{58}$$

where $A_{i,u_{i\vartheta}} = \frac{\partial A_i(u_i)}{\partial u_i}|_{u_i = u_{i\vartheta}}$ and $u_{i\vartheta} = \vartheta_i u_i + (1 - \vartheta_i)u_{i0}$. Let $u_{i0} = 0$, then it can be derived that

$$A_i(u_i) = A_{i,u_{i\vartheta}} u_i \tag{59}$$

where $A_{i,u_{i\vartheta}}$ is positive and bounded from $\mathcal{S}(.)$ in (55)

$$A_{i,u_{i\vartheta}} = 2a_0 \frac{e^{-\frac{a_0 u_i}{u_{iM}}}}{(e^{-\frac{a_0 u_i}{u_{iM}}} + 1)^2} \leq 2a_0 \tag{60}$$

Then the observer (10)-(11) can be turned into

$$\dot{\hat{x}}_{i,m} = \hat{x}_{i,m+1} - l_{i,m}(\hat{x}_{i,1} - y_i) \tag{61}$$
$$\dot{\hat{x}}_{i,n_i} = A_{i,u_{i\vartheta}} u_i - l_{i,n_i}(\hat{x}_{i,1} - y_i) \tag{62}$$

where $m = 1, ..., n_i - 1$.

The observer errors (14)-(15) are reformed as

$$\dot{e}_{i,m} = -l_{i,m}e_{i,1} + e_{i,m+1} + f_{i,m}(x_i) + g_{i,m}(y) + h_{i,m}(y_{\tau_{i,m}}) \tag{63}$$
$$\dot{e}_{i,n_i} = -l_{i,n_i}e_{i,1} + \Delta_i(u_i) + f_{i,n_i}(x_i) + g_{i,n_i}(y) + h_{i,n_i}(y_{\tau_{i,n_i}}) \tag{64}$$

which can be expressed as the following form

$$\dot{e}_i = A_{i,c}e_i + F_i(x_i) + G_i(y) + H_i(y_{\tau_i}) + \Pi_i(u_i) \tag{65}$$

where $e_i = [e_{i,1}, \ldots, e_{i,n_i}]^T$, $F_i(x_i) = [f_{i,1}(x_i), \ldots, f_{i,n_i}(x_i)]^T$, $G_i(y) = [g_{i,1}(y), \ldots, g_{i,n_i}(y)]$, $H_i(y_{\tau_i}) = [h_{i,1}(y_{\tau_{i,1}}), \ldots, h_{i,n_i}(y_{\tau_{i,n_i}})]^T$, $\Pi_i(u_i) = [0, ..., 0, \Delta_i(u_i^s)]^T$.

The design steps of the distributed tracking controller with input saturation are the same as that without saturation, thus step n_i can be re-derived.

Step n_i: The distributed fault tolerant control input can be designed by

$$\begin{aligned} u_i = \frac{1}{2a_0}(&\dot{\alpha}_{i,n_i-1} - z_{i,n_i-1} - b_{i,n_i}z_{i,n_i} - l_{i,n_i}e_{i,1} - \frac{1}{2}z_{i,n_i} \\ &-\frac{2}{z_{i,n_i}}(\tanh^2(z_{i,n_i}/\varsigma)(\gamma_i^s + \hat{\eta}_i^s))) \end{aligned} \tag{66}$$

where $\hat{\eta}_i^s = \hat{W}_i^T\varphi_i$ is the estimation of the unknown dynamics η_i^s, $\eta_i^s = \eta_i + (A_{i,u_{i\vartheta}} - 2a_0)z_{i,n_i}u_i$, $\gamma_i^s = \gamma_i + 16\beta u_{iM}^2 + 16u_{iM}^2$, γ_i, η_i, $\hat{W}_i$ are given in (43) and (45).

Computing the derivative of (17) leads to

$$\begin{aligned} \dot{V}_i^1 \le& -\frac{1}{2}e_i^TQ_ie_i + \beta\sum_{j=1}^{n_i} f_{i,j}^T(x_i)f_{i,j}(x_i) - \chi_iV_{h_i} + N\beta\sum_{j=1}^{n_i}\sum_{k=1}^{N} 2\breve{\phi}_{i,j,k}^2(y_k) \\ &+N\beta\sum_{j=1}^{n_i}\sum_{k=1}^{N} 2\bar{\phi}_{i,j,k}^2(y_k) + \frac{N\beta}{1-d_i^*}\sum_{j=1}^{n_i} e^{\chi_i\bar{d}_i}\left(\sum_{k=1}^{N} 2\breve{\omega}_{i,j,k}^2(y_k)\right) + 4\delta e_i^2||P_i||^2 \\ &+\frac{N\beta}{1-d_i^*}\sum_{j=1}^{n_i} e^{\chi_i\bar{d}_i}\left(\sum_{k=1}^{N} 2\bar{\omega}_{i,j,k}^2(y_k)\right) + 16\beta u_{iM}^2 \end{aligned} \tag{67}$$

where δ and β are defined as (20).

Computing the derivative of (40) leads to

$$\dot{V}_i^2 \le \dot{V}_{i,n_i-1}^2 + \frac{1}{4}z_{i,n_i}^2 + 16u_{iM}^2 + z_{i,n_i}(2a_0u_i + l_{i,n}e_{i,1} - \dot{\alpha}_{i,n-1} + (A_{i,u_{i\vartheta}} - 2a_0)u_i) \tag{68}$$

Choosing a positive definite matrix Λ_i such that $Q_i = 8\delta||P_i||^2I_{n_i} + 2\Lambda_i$, then $\dot{V}_i$ is transformed into

$$\begin{aligned} \dot{V}_i = \dot{V}_i^1 + \dot{V}_i^2 \le& -(\chi_i - \frac{1}{2})e_i^2 + 2\tanh^2(z_{i,n_i}/\varsigma))(\gamma_i^s + \eta_i^s) - 2\chi_iV_{h_i} + z_{i,n_1-1}^Tz_{i,n_i} \\ &-\sum_{c=2}^{n_i-1} b_{i,c}z_{i,c}^2 + z_{i,n_i}(2a_0u_i + l_{i,n}e_{i,1} - \dot{\alpha}_{i,n-1}) - (b_{i,1} - \frac{3}{2})z_{i,1}^2 \\ &+\frac{1}{4}z_{i,n_i}^2 + (1 - 2\tanh^2(z_{i,n_i}/\varsigma))(\gamma_i^s + \eta_i^s) \end{aligned}$$

From (66), one has

$$\begin{aligned}\dot{\bar{V}}_i = \dot{V}_i - \varrho_i \tilde{W}_i^T \dot{\hat{W}}_i \le -(\chi_i - \frac{1}{2})e_i^2 - 2\chi_i V_{h_i} - (b_{i,1} - \frac{3}{2})z_{i,1}^2 \\ - \sum_{c=2}^{n_i} b_{i,c} z_{i,c}^2 - \frac{\lambda_i}{2}\tilde{W}_i^2 + \frac{\lambda_i}{2}W_i^2 - \frac{1}{4}z_{i,n_i}^2 + 2\tanh^2(z_{i,n_i}/\varsigma)\bar{\epsilon} \\ +(1 - 2\tanh^2(z_{i,n_i}/\varsigma))(\gamma_i^s + \eta_i + (A_{i,u_{i\vartheta}} - 2a_0)z_{i,n_i}u_i)\end{aligned} \tag{69}$$

Therefore, the closed loop INS and the design procedure could be illustrated as Figure 3 and Figure 4.

Based on the above descriptions, the second result is now ready to be presented.

Theorem 2. Consider the interconnected systems (9) with input saturation constraints (54), under Assumptions 1-3, the designed distributed tracking controller (66) and the adaptive parameter update algorithm (45) guarantee that the closed-loop interconnected systems are uniformly ultimate bounded stable, meanwhile all the tracking errors are uniformly ultimately bounded.

Proof: The Lyapunov candidate function is chosen as $V = \sum_{i=1}^{N} \bar{V}_i$. For $(A_{i,u_{i\vartheta}} - 2a_0)u_i$ is bounded, one yields due to Lemma 1

$$\begin{aligned}\dot{V} \le \sum_{i=1}^{N}(-(\chi_i - \frac{1}{2})e_i^2 - 2\chi_i V_{h_i} - (b_{i,1} - \frac{3}{2})z_{i,1}^2 - \sum_{c=2}^{n_i} b_{i,c} z_{i,c}^2 - \frac{\lambda_i}{2}\tilde{W}_i^2 + 2\tanh^2(z_{i,n_i}/\varsigma)\bar{\epsilon} \\ - \frac{1}{4}z_{i,n_i}^2 + \frac{\lambda_i}{2}W_i^2 + \bar{A}_{i,u_{i\vartheta}}|z_{i,n_i}| - 2\tanh^2(z_{i,n_i}/\varsigma))/z_{i,n_i}(A_{i,u_{i\vartheta}} - 2a_0)u_i z_{i,n_i}^2) \\ \le -\mu V + M^s\end{aligned} \tag{70}$$

where $|(A_{i,u_{i\vartheta}} - 2a_0)u_i| \le \bar{A}_{i,u_{i\vartheta}}$ and $\bar{A}_{i,u_{i\vartheta}}$ is a positive constant. $M_0^s = M_0 + \bar{A}_{i,u_{i\vartheta}}^2$, $|M_0^s| \le M^s$, and M^s is a positive constant. If $b_{i,n_i} \ge -2\tanh^2(z_{i,n_i}/\varsigma))/z_{i,n_i}(A_{i,u_{i\vartheta}} - 2a_0)u_i$ and μ is chosen as (49), then the inequality (70) holds.

According to (70), it can be concluded that $e_{i,j}$, $z_{i,j}$, $\tilde{W}_i$ $(i = 1, ..., N;\ j = 1, \dots, n_i)$ of the interconnection systems (9) are UUB and simultaneously the whole closed loop INS are uniformly ultimate bounded stable. From (70), the output tracking error $z_{i,1}$ is adjusted into a small region near origin by selecting the proper parameters $b_{i,j} > 0$, $\lambda_i > 0$, $\varsigma > 0$ and $\varrho_i > 0$. Namely, the larger μ and smaller M^s, the better control performance of (9). Note that χ_i in saturation case should be smaller than that in normal case when Q_i and δ are selected as the same in both cases. The proof is completed.

Remark 6: From (70), it is easily known that the larger $b_{i,j}$, λ_i, ς and smaller ϱ_i, the better control performance of (9). In the actual application, these parameters need to be tried many times and adjusted carefully to obtain the appropriate values for achieving the satisfactory control performance. Meanwhile, the related parameters in the design procedure could be chosen according to the given parameter selection guideline.

1) Specify the known positive constants $d_{i,j}, c_1, c_2, c_3, a_0, \bar{\epsilon}_i$ to the controlled systems (9).

2) Choose the appropriate gain parameter $l_{i,j}$ such that $A_{i,c}$ of (65) be a strict Hurwitz matrix.

3) Choose the appropriate parameters such that $b_{i,c} > 0,\ \varsigma > 0,\ \lambda_i > 0,\ \varrho_i > 0$, which

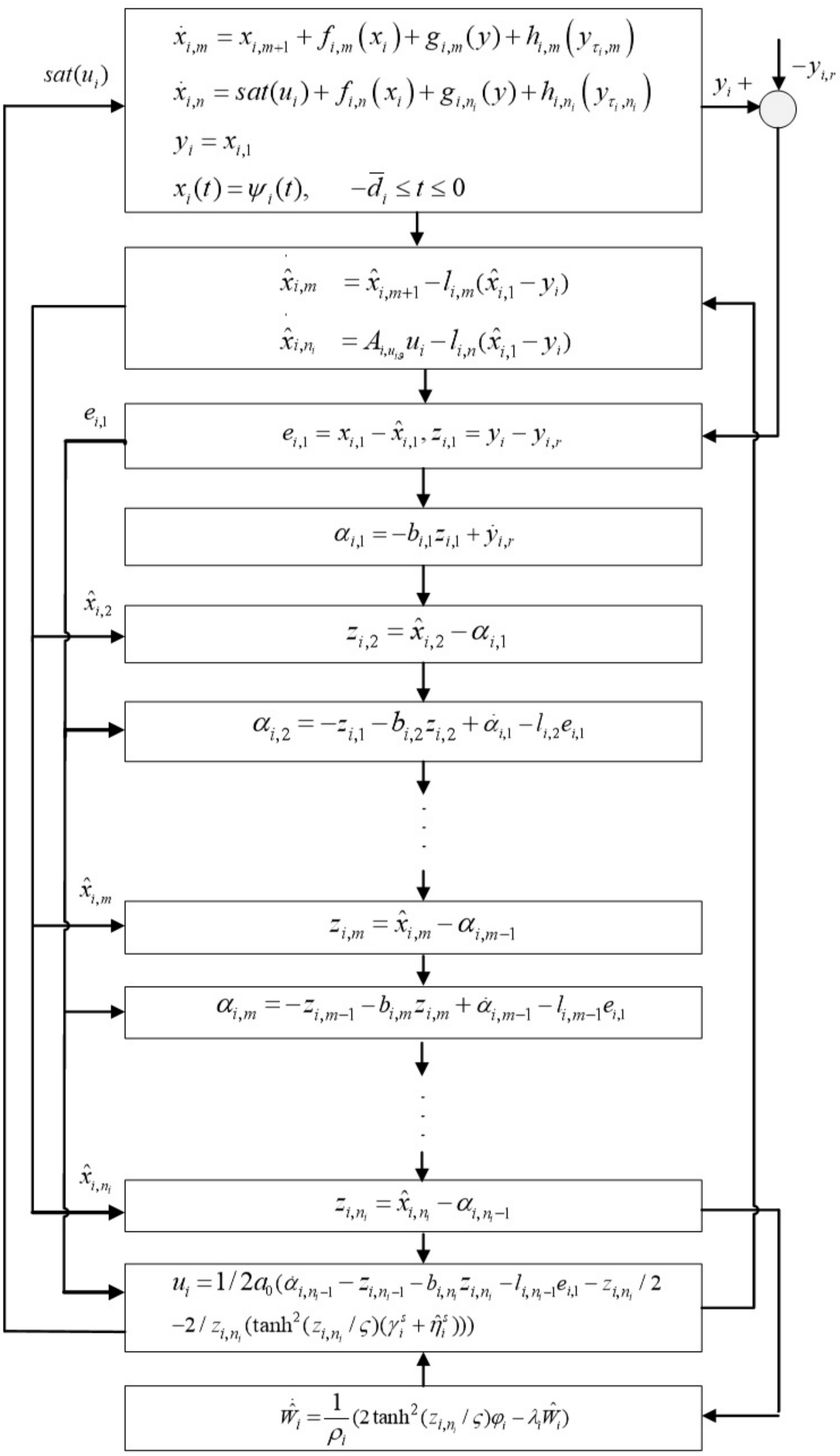

Figure 4. Block diagram of the design procedure

determine the virtual control input, the actual control input in (66) and the adaptive parameter update algorithm in (45).
4) Ensure that the parameters selected above could make the inequality (70) hold.

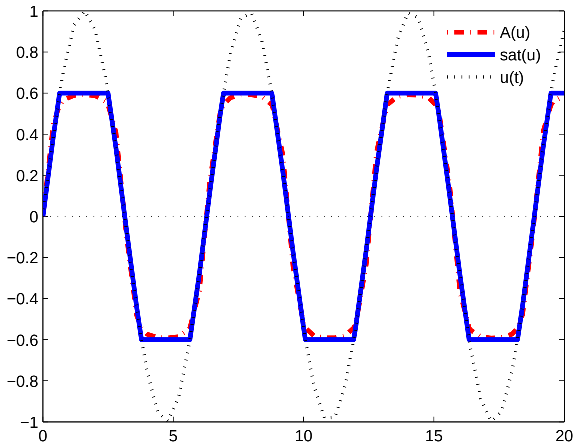

Figure 5. Curve of the input saturation approximation ($a_0 = 3$).

Remark 7: The decentralized control scheme of INS is developed in (Liu, 2019; Ma & Ma, 2020; Sun & Zong, 2020; Wang & Yang, 2019; Zhang, 2020) and (Tong, 2011), in which only the local subsystem information is adopted and only the stability of local subsystem is guaranteed. Different from these results, the DC scheme of INS is employed in this paper for practical engineering applications, it fully utilizes neighbor subsystems information such that the stability of the whole closed-loop INS is obviously improved.

Remark 8: Although the distributed tracking control problem has been investigated in (Yoo, 2016), the time delay interconnections, input saturations and unmeasured states are not taken into account. In this paper, all these problems described above are studied for the considered INS. Therefore, this study has wider applications than some existing results, it could be regarded as the expansion and improvement of the results developed in (Yoo, 2016).

Remark 9: When the order of considered systems is high, the differential explosion in the calculation of partial derivatives of virtual control variables may occur in above Theorems 1 and 2. In order to avoid "differential explosion", the instruction filtering or low pass filter can be introduced into the backstepping control method (Tong, 2011).

4. Simulation Example

In this section, the stability and robustness of the INS will be considered as a case study to demonstrate the theoretical results. Two inverted double pendulum cars connected by a spring shown in Figure 6 can be described by (Sun & Hou, 2020) and (Baigzadehnoe, 2020).

$$\begin{cases} \dot{x}_{i,1} = x_{i,2} + f_{i,1}(x_i) + g_{i,1}(y) + h_{i,1}(y_{\tau_{i,1}}) \\ \dot{x}_{i,2} = \frac{u_i}{J_i} + f_{i,2}(x_i) + g_{i,2}(y) + h_{i,2}(y_{\tau_{i,2}}) \\ y_i = x_{i,1}, \;\; i = 1, 2 \end{cases} \tag{71}$$

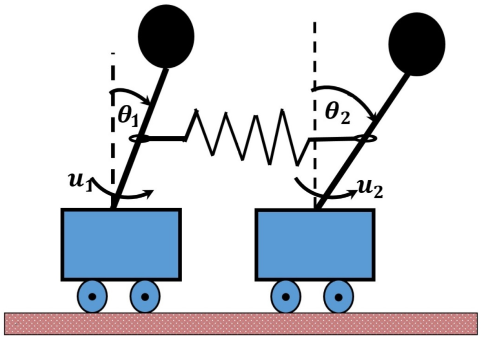

Figure 6. Parallel inverted pendulum cars

where $x_i = [x_{i,1}, x_{i,2}]^T = [\theta_i, \dot{\theta}_i]^T$ respectively denote the angular displacement and angular velocity of the pendulums from vertical. $f_{i,1}(x_i) = 0$, $f_{i,2}(x_i) = \frac{m_i gr}{J_i} - \frac{kr^2}{4J_i} sin(x_{i,1})$, $g_{i,1}(y) = 0$, $g_{1,2}(y) = \frac{kr}{2J_1}(l-b) + \frac{kr^2}{4J_1} sin(y_2)$, $g_{2,2}(y) = \frac{kr}{2J_2}(l-b) + \frac{kr^2}{4J_2} sin(y_1)$. To increase the complexity of time-delay interconnected systems (74), the nonlinear interconnection terms with delays are chosen as $h_{i,1}(y_{\tau_{i,1}}) = 0$, $h_{1,2}(y_{\tau_{1,2}}) = \frac{1}{J_1}(y_1^2(t-d_{1,2}) * cos(y_1(t-d_{1,2}))) + \frac{1}{J_2}(y_2(t-d_{1,2}) * sin(y_2(t-d_{1,2})))$, $h_{2,2}(y_{\tau_{2,2}}) = \frac{1}{J_2}(y_2^2(t-d_{2,2}) * cos(y_2(t-d_{2,2}))) + \frac{1}{J_1}(y_1(t-d_{2,2}) * sin(y_1(t-d_{2,2})))$. Here m_1 and m_2 denote the pendulum end masses, J_1 and J_2 are the inertia moments, k denotes the spring constant, r is the pendulum height, l means the spring natural length, b is distance between the pendulum hinges, and g is the gravitational acceleration. According to (Sun & Hou, 2020), the system parameters are given as $m_1 = 2$kg, $m_2 = 2.5$kg, $J_1 = 5$kg, $J_2 = 6.25$kg, $k = 100$N/m, $g = 9.81$m/s^2, $r = 0.5$m, $l = 0.5$m, $b = 0.5$m. The time varying delays are selected as $d_{1,2} = 0.1 + 0.1cos(0.5t)$, $d_{2,2} = 0.2 - 0.2sin(0.5t)$, then $\bar{d}_1 = 0.2$, $\bar{d}_2 = 0.4$.

The reference signals are given as $y_{1,r} = 0.8cos(t-0.5) + 0.3sin(4t)$ and $y_{2,r} = 0.7sin(t) - 0.4cos(3t)$. The initial condition is chosen as $x_{1,1}(0) = 0.5$, $x_{2,1}(0) = 0.5$, $\hat{x}_{1,1}(0) = \hat{x}_{2,1}(0) = 0$, $\psi_1(t) = \psi_2(t) = 0.2[cos(t);\ sin(t)]$ with $t \in [-0.4, 0]$.

To illustrate the effectiveness of the distributed control (DC) scheme, two different cases will be carried out in the simulation as follows.

Case 1: The interconnected nonlinear systems (INS) with time-delay interconnections, unmeasured states are investigated in this case. First, a nonlinear state observer is introduced and then the distributed controller is developed according to Theorem 1. The designed parameters are selected as $l_{1,1} = 4$, $l_{1,2} = 1.75$, $l_{2,1} = 5$, $l_{2,2} = 2$, $\delta = 0.01$, $\chi_1 = 0.79$, $\chi_2 = 0.587$, $\varrho_1 = \varrho_2 = 10$, $b_{1,1} = b_{2,1} = 10$, $b_{1,2} = b_{2,2} = 5$, $\lambda_1 = \lambda_2 = 1$.

Case 2: The INS with time-delay interconnections, unmeasured states and input saturations are discussed in this case. Similarly, we design a state observer and then a distributed controller according to Theorem 2. The designed parameters are selected as $l_{1,1} = 4$, $l_{1,2} = 1.75$, $l_{2,1} = 5$, $l_{2,2} = 2$, $\delta = 0.01$, $\chi_1 = 0.6$, $\chi_2 = 0.134$, $\varrho_1 = \varrho_2 = 5$, $b_{1,1} = b_{2,1} = 5$, $b_{1,2} = b_{2,2} = 2$, $\lambda_1 = \lambda_2 = 1$, $u_{1M} = 35$, $u_{2M} = 40$.

The broad learning system is introduced to estimate the unknown dynamics online. At initialization time, the weight parameters of BLS are random from $[-1, 1]$, just as shown in Table I, and then their online training and updating run according to Table II and (45). Due to the characteristics of the systems (71), the activation function $\zeta_1(x) = x$, and $\zeta_2(x) = \tanh(x) = \frac{e^x - e^{-x}}{e^x + e^{-x}}$.

In Figure 7, the original outputs y_1, y_2 of both inverted pendulums and their de-

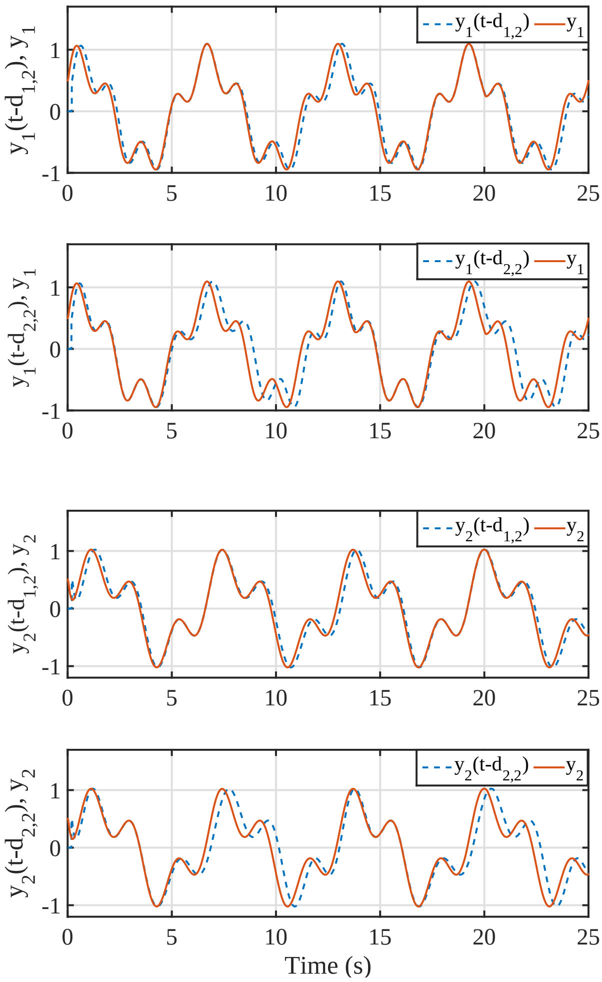

Figure 7. Curves of output signals in CASE 1

layed outputs generated by $d_{1,2}$ and $d_{2,2}$ between the first and second car are displayed. It is easily known from the preset conditions that the amplitude of $d_{2,2}$ is larger than that of $d_{1,2}$, so the phase deviations between $y_i(t-d_{2,2})$ and y_i $(i=1,2)$ are obviously larger than that between $y_i(t-d_{1,2})$ and y_i in Figure 7. The state observer (10)-(11) can accurately estimate the states $\hat{x}_{1,1}$, $\hat{x}_{1,2}$, $\hat{x}_{2,1}$, $\hat{x}_{2,2}$ as shown in Figure 8. It is clear that in CASE 1 the outputs of both inverted pendulums can track the desired trajectory y_{1r}, y_{2r} and their tracking errors nearly converge to a very small neighborhood of zero as exhibited in Figures 9-10. However, the control inputs in Figure 9 are too large to be allowed in the practical systems due to energy or amplitude limitations of actuators. Thus, the distributed control scheme for the uncertain time-delay INS should be further improved, that is, the input saturation constraints have to be taken into account next.

Similarly in CASE 2, it is shown in Figure 12 that the state observer could accurately approach the states of two inverted pendulums. Although in Figures 13-14 it is clearly demonstrated that the input saturation will degrade the dynamical tracking performance of the systems (71) in CASE 2, the tracking trajectory steady-state errors can still reach in a small neighborhood of zero and the steady-state precision in CASE 2

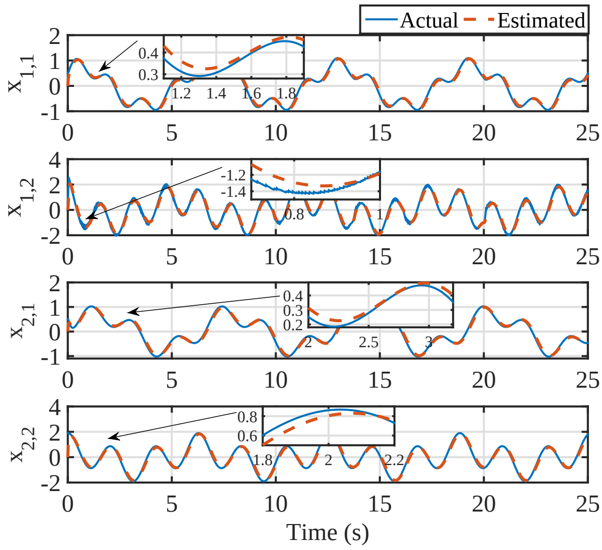

Figure 8. Curves of estimated states in CASE 1

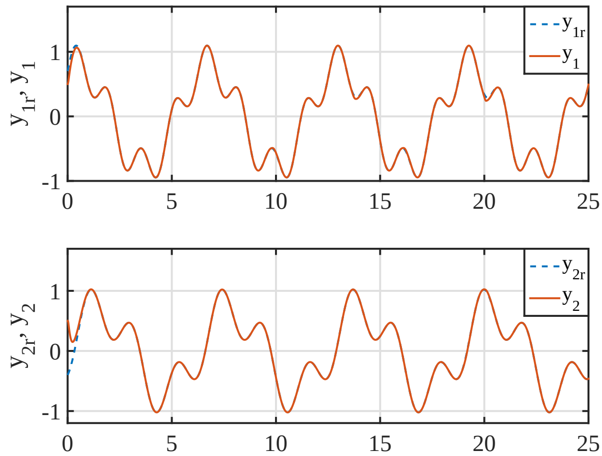

Figure 9. Curves of tracking signals in CASE 1

nearly equals to CASE 1. Moreover, the control inputs of both inverted pendulums are limited within the bounds just as shown in Figure 15, which is available in the practical systems. And it is clear that the bounds of the control inputs are $u_{1M} = 35$, $u_{2M} = 40$, which is the same as the preset bounds.

In conclusion, the above simulation results demonstrate that the developed distributed control approach is valid and feasible for the considered nonlinear multi-delay systems in presence of inaccessible states and input saturations.

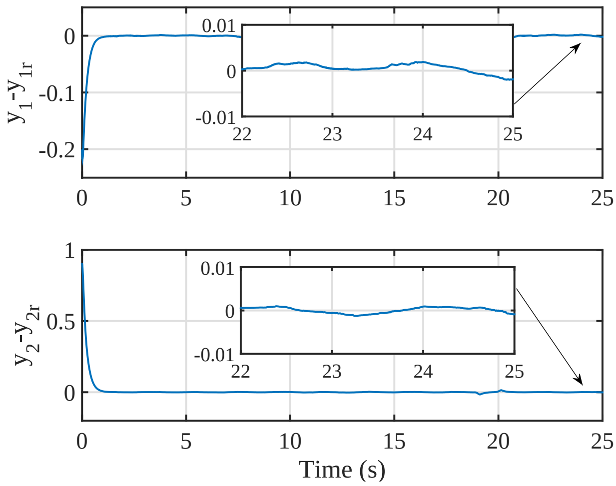

Figure 10. Curves of tracking errors in CASE 1

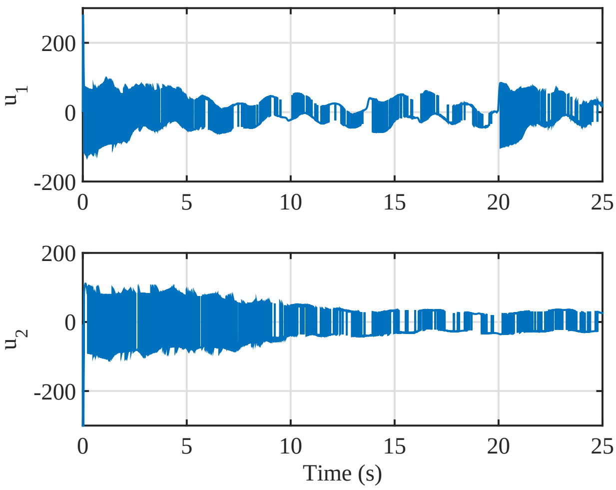

Figure 11. Curves of control inputs in CASE 1

5. Conclusion

In this paper, a BLS-based distributed adaptive tracking control scheme is proposed for time-delay interconnected nonlinear systems (INS) with input saturations. A full dimension state observer is designed to estimate the inaccessible state variables, and then a distributed adaptive tracking control scheme (DATC) is proposed with the help of BLS technique. Meanwhile the stability of the time-delay INS without input saturations is analyzed. To solve the input saturation problem, a well defined smooth function is introduced into the improved DATC, which guarantees the stability of the closed loop INS with input saturations. Finally, the simulation results are given to illustrate the effectiveness of the proposed control strategy. In addition, the DATC will be extended to the time-delay INS with full state constraints in our future work.

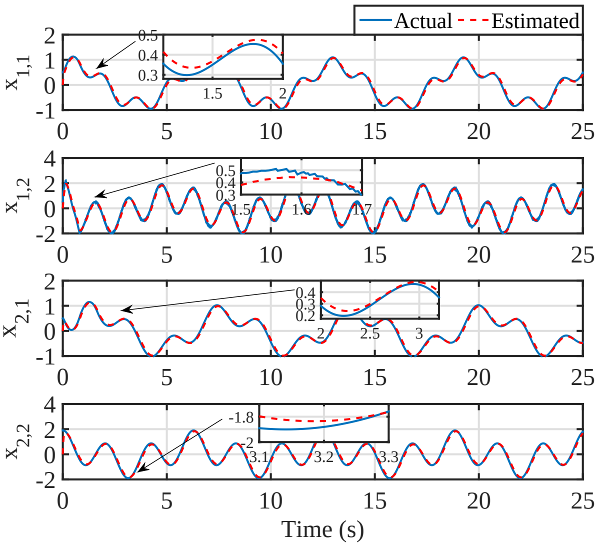

Figure 12. Curves of estimated states in CASE 2

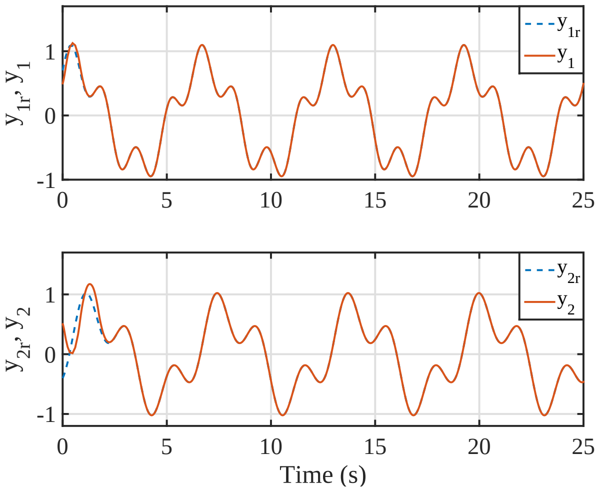

Figure 13. Curves of tracking signals in CASE 2

Acknowledgement(s)

The authors also gratefully acknowledge the helpful comments and suggestions of the reviewers, which helped to improve the quality of this paper.

Disclosure statement

The authors declare that there is no conflict of interest in relation to this article.

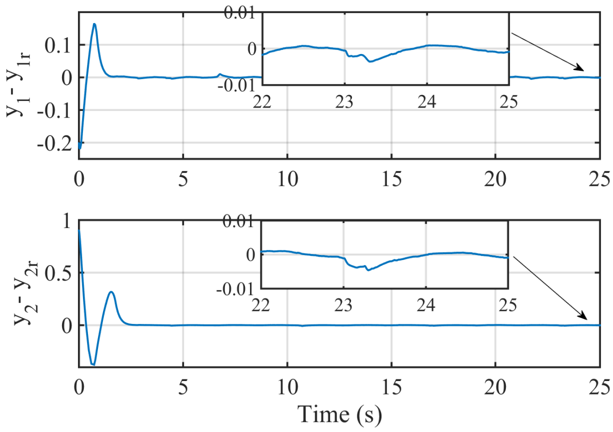

Figure 14. Curves of tracking errors in CASE 2

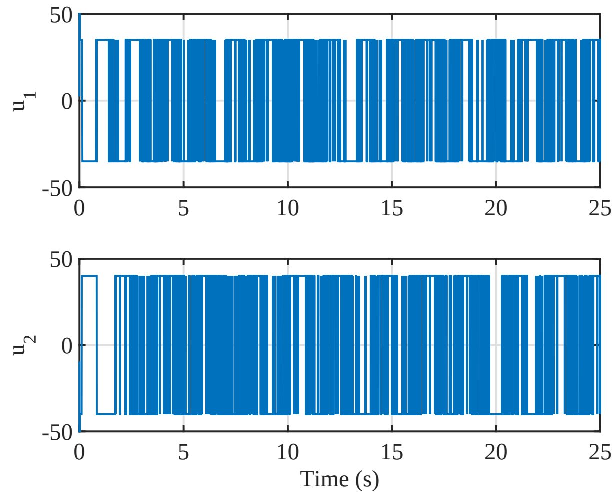

Figure 15. Curves of control inputs in CASE 2

Data Availability Statement

The data used to support the findings of this study are available from the corresponding author upon request.

Funding

This work was supported by the National Natural Science Foundation of China (62333010), National Key Research and Development Program of China (2022YF-B3305300).

References

Apostol, T. M., & Ablow, C. M. (1958). Mathematical analysis. *Physics Today*, *11*(7), 32.

Baigzadehnoe, B., Rahmani, Z., Khosravi, A., & Rezaie, B. (2020). Adaptive decentralized fuzzy dynamic surface control scheme for a class of nonlinear large-scale systems with input and interconnection delays. *European Journal of Control*, *54*(7), 33–48.

Chen, Z. H., Cheng, J., Tan, J., & Cao, Z. (2020). Decentralized finite-time control for linear interconnected fractional-order systems with input saturation. *Journal of the Franklin Institute*, *357*, 6137–6153.

Chen, C. L. P., & Liu, Z. L. (2018). Broad learning system: An effective and efficient incremental learning system without the need for deep architecture. *IEEE Transactions on Neural Networks and Learning Systems*, *29*(1), 10–24.

Chen, C. L. P., Liu, Z. L., & Feng, S. (2019). Universal approximation capability of broad learning system and its structural variations. *IEEE Transactions on Neural Networks and Learning Systems*, *30*(4), 1191–1204.

Chu, F., Liang, T., Chen, C. L. P., Wang, X. S., & Ma. X. P. (2020). Weighted broad learning system and its application in nonlinear industrial process modeling. *IEEE Transactions on Neural Network and Learning Systems*, *31*(8), 3017–3031.

Cui, D., Niu, B., Wang, H.Q., Yang, D. (2019). "Adaptive neural tracking control of nonlinear stochastic switched non-lower triangular systems with input saturation." *Neurocomputing*, *364*, 192-202.

Ghosh, S., Das, S. K., & Ray, G. (2009). Decentralized stabilization of uncertain systems with interconnection and feedback delays: an LMI approach. *IEEE Transactions on Automatic Control*, *54*(4), 905–912.

Li, D. J., Li. D. P. (2018). Adaptive tracking control for nonlinear time-varying delay systems with full state constraints and unknown control coefficients. *Automatica*, *93*, 444–453.

Li, X. J., & Yang, G. H. (2018). Neural-network-based adaptive decentralized fault-tolerant control for a class of interconnected nonlinear systems. *IEEE Transactions on Neural Networks and Learning Systems*, *29*(1), 144–155.

Liu, C., Zhang, H. G., Xiao, G. Y., & Sun, S. X. (2019). Integral reinforcement learning based decentralized optimal tracking control of unknown nonlinear large-scale interconnected systems with constrained-input. *Neurocomputing*, *323*(1), 1–11.

Li, Y., Li, Y. X., Tong, S. C. (2023). "Event-Based Finite-Time Control for Nonlinear Multiagent Systems With Asymptotic Tracking." *IEEE Transactions on Automatic Control*, *68*(6), 3790-3797, June 2023, doi: 10.1109/TAC.2022.3197562.

Liu, X. M., Xia, J. W., Wang, J., & Shen, H. (2020). Interval type-2 fuzzy passive filtering for nonlinear singularly perturbed PDT-switched systems and its application. *Journal of Systems Science and Complexity*, *34*, 2195–2218.

Li, Y. M., Zheng, X., & Li, K. (2023). Prescribed-Time Adaptive Intelligent Formation Controller for Nonlinear Multi-Agent Systems Based on Time-Domain Mapping. *IEEE Transactions on Artificial Intelligence*. doi: 10.1109/TAI.2023.3299439.

Ma, Z. Y., & Ma, H. J. (2020). Decentralized adaptive NN output-feedback fault compensation control of nonlinear switched large-scale systems with actuator dead-zones. *IEEE Transactions on Systems. Man. and Cybernetics: Systems*, *50*(9), 3435–3447.

Mu, J. Q., Yan, X. G., Spurgeon, S. K., & Zhao, D. Y. (2018). Nonlinear sliding mode control for interconnected systems with application to automated highway systems. *IEEE Transactions on Control of Network Systems*, *5*(1), 664–674.

Niu, B., Liu, J., Duan, P., Li, J., Yang, D. (2021). "Reduced-Order Observer-Based Adaptive Fuzzy Tracking Control Scheme of Stochastic Switched Nonlinear Systems." *IEEE Transactions on Systems, Man, and Cybernetics: Systems*, *51*(7), 4566-4578, July 2021, doi: 10.1109/TSMC.2019.2943882.

Salari, M. E., Coleman, J., & Toal, D. (2019). Analysis of direct interconnection technique for offshore airborne wind energy systems under normal and fault conditions. *Renewable Energy*, *131*, 284–296.

Sui, S., Chen, C. L. P., Tong, S. C., & Feng, S. (2020). Finite-time adaptive quantized control of stochastic nonlinear systems with input quantization: A broad learning system based identification method. *IEEE Transactions on Industrial Electronics*, *67*(10), 8555–8565.

Sun, H. B., Hou, L. L., Zong, G. D., & Yu, X. H. (2020). Adaptive decentralized neural network tracking control for uncertain interconnected nonlinear systems with input quantization and time delay. *IEEE Transactions on Neural Networks and Learning Systems*, *31*(4), 1401–1409.

Sui, S., Philip Chen, C. L., & Tong, S. C. (2021) A Novel Adaptive NN Prescribed Performance Control for Stochastic Nonlinear Systems. *IEEE Transactions on Neural Networks and Learning Systems*, *32*(7). 3196–3205.

Sun, H. B., Zong, G. D., & Philip Chen, C. L. (2020). Adaptive decentralized output feedback PI tracking control design for uncertain interconnected nonlinear systems with input quantization. *Information Sciences*, *512*, 186–206.

Tong, S., Li, Y. M., & Zhang, H. G. (2011). Adaptive neural network decentralized backstepping output-feedback control for nonlinear large-scale systems with time delays. *IEEE Trans. Neural Netw*, *22*(7), 1073–1086.

Wang, C. C., & Yang, G. H. (2019). Event-triggered decentralized output-feedback control for interconnected nonlinear systems with input quantization. *Journal of the Franklin Institute*, *356*, 7028–7048.

Wang, J., Xia, J. W., & Shen, H. (2020). H_∞ synchronization for fuzzy markov jump chaotic systems with piecewise-constant transition probabilities subject to pdt switching rule. *IEEE Transactions on Fuzzy Systems*, *29*(10), 3082–3092.

Wang, J., Yang, C. Y., Xia, J. W., Wu, Z. G., & Shen, H. (2021). Observer-based sliding mode control for networked fuzzy singularly perturbed systems under weighted try-once-discard protocol. *IEEE Transactions on Fuzzy Systems*, *30*(6), 1889–1899.

Yan, X. H., Chen, M., Feng, G., Wu, Q. X., & Shao, S. Y. (2021). Fuzzy robust constrained control for nonlinear systems with input saturation and external disturbances. *IEEE Transactions on Fuzzy Systems*, *29*(2), 345–356.

Yang, H., Huang, C. K., Jiang, B., & Polycarpou, M. M. (2019). Fault estimation and accommodation of interconnected systems: a separation principle. *IEEE Transactions on Cybernetics*, *49*(12), 4103–4116.

Yoo, S. J. (2016). Distributed memoryless detection and accommodation of unknown time-delayed interaction faults in a class of interconnected nonlinear systems. *Information Sciences*, *329*(2), 753–764.

Yu, Z. Q., Qu, Y. H., & Zhang, Y. M. (2019). Distributed fault-tolerant cooperative control for Multi-UAVs under actuator fault and input saturation. *IEEE Transactions on Control Systems Technology*, *27*(6), 2417–2429.

Zhang, K., Jiang, B., Chen, M., & Yan, X. G. (2019). Distributed fault estimation and fault-tolerant control of interconnected systems. *IEEE Transactions on Cybernetics*, *51*(3), 1230–1240.

Zhao, K., Song, Y. D., Chen, C. L. P., & Chen, L. (2020). Control of nonlinear systems under dynamic constraints: A unified barrier function-based approach. *Automatica*, *119*(109102), 1–9.

Zhang, L. L., Hua, C. C., Cheng, G. Y., Li, K., & Guan, X. P. (2020). Decentralized adaptive output feedback fault detection and control for uncertain nonlinear interconnected systems. *IEEE Transactions on Cybernectics*, *50*(3), 935–945.

Zhang, J., & Xiang, Z. R. (2022). Event-triggered adaptive neural network sensor failure compensation for switched interconnected nonlinear systems with unknown control coefficients. *IEEE Transactions on Neural Networks and Learning Systems*, *33*(10), 5241–5252.

Zhang, Q., Dong, & J. X. (2020). Disturbance-observer-based adaptive fuzzy control for nonlinear state constrained systems with input saturation and input delay. *Fuzzy Sets and Systems*, *392*, 77–92.

Zhan, Y., Sui, S., & Tong, S. (2021). Adaptive Fuzzy Decentralized Control for Fractional-Order Interconnected Nonlinear Systems with Input Saturation. *International Journal of Systems Science*, *52*(13), 2689-2703.